COPPER VAPOR LASER
SCALE DEMONSTRATION

FINAL REPORT

October 1981 to February 1983

Prepared for

Office of Naval Research

Contract N00014-82-C-0057

Prepared by

T. W. Karras
M. H. Bortner
C. E. Anderson

Sponsored in part by

Defense Advanced Research Projects Agency
DARPA ORDER NO. 3650 Amendment #19

General Electric Company
SPACE DIVISION
P. O. Box 8555
Philadelphia, PA 19101

COPPER VAPOR LASER

SCALE DEMONSTRATION

FINAL REPORT

by

T. W. KARRAS
M. H. BORTNER
C. E. ANDERSON

General Electric Company
SPACE DIVISION

(215) 962-4658

Prepared for

Office of Naval Research

Technical Monitor: M. White

ABSTRACT

A pulsed copper vapor laser has been successfully scaled to 10 cm diameter.

A computer simulation model of the pulsed copper vapor laser in both helium and neon buffers was developed and validated. It projects output pulse energy at 510.5 nm of over 0.33 joules and efficiency of over 2.5% from a 10 cm diameter laser running at 200 HZ, in neon.

The key to such operation is the decay of ionization and gas heating during the long interpulse period and the application of high voltage for reliable breakdown. This minimizes skin effect limitations and increases electron temperature.

A flexible large bore laser test facility was built using glow discharge heating and burst mode excitation. Preliminary tests with a 4 1/8" diameter laser were fully successful. Glow discharges could heat the laser to the 1400°C-1500°C range and pulsed discharges filled the full bore. Pulse to pulse reproducibility could be achieved at 200 HZ after only two pulses if voltages of 36 KV were applied to the storage capacitor. The specific loading in these tests was several millijoules per cm³, the range projected by the model as necessary for high energy output.

Laser operation was also demonstrated filling essentially the full bore. Estimates of unoptimimized output energy in helium were in the range of >70 millijoules, the highest ever reported from a pulsed metal vapor laser. These results were consistent with computer simulations. Measured current and voltage waveforms agreed very closely with computer generated plots.

ACKNOWLEDGEMENTS

The authors would like to acknowledge the aid of George Bethke, John DiLello, and John Medved in design of the laser; Albert Kreft and Peter Parkinson during laser assembly and shakedown testing; Louis Springer for electronics design, set-up and test; George Bethke and Daniel Stern in computer modeling, and most of all Bernard Fox, for yeoman service throughout the program.

TABLE OF CONTENTS

LIST OF ILLUSTRATIONS

LIST OF TABLES

I. INTRODUCTION

Copper vapor lasers have long been considered a promising source for moderate average power in the visible parts of the spectrum. However, most studies have focused upon repetition rates above 1 KHZ and pulse energies limited to, at most, a few tens of millijoules. With the advent of large bore devices and the repeated demonstration of high average power it has been suggested that hundreds of millijoules could be produced from a large device operating at low repetition rates.[1]

An emperical projection identified the size and characteristics a copper vapor oscillator would have to have if it were to produce about .25 joules. In particular it was noted that a specific output of 25 $\mu J/cm^3$ could be produced if specific loading of 2 - 2.5 mJ/cm^3 was applied. Then a 4" ID active medium of 100-150 cm length would suffice. Other considerations, such as plasma shielding of the tube axis, discharge stability etc. were also discussed supporting the practicality of a test.

The following report describes the development of a computer simulation model supporting these empirical projections and the design, construction, and preliminary test of a flexible large bore laser facility that verifies them through experiment in a 4" bore device.

II. REGIME OF OPERATION

Laser operation in neutral copper vapor, as in other media of this class, is inherently pulsed or self-terminated because the lower laser state is metastable. No mechnism for depopulating this state concurrently with excitation of the upper laser state has yet been found. Thus, the basic process has a cyclic pattern. A fast electrical discharge pulse produces an inversion, and this is followed sequentially by laser oscillation and an extended period during which the metastable lower state must relax before the cycle can be repeated.[2]

The nature of this operation can be easily seen by referring to the energy level diagram of the copper atom shown in Figure 1. The upper laser states (4^2P) are excited from the ground state by direct electron collisions. These levels are resonant states which are strongly coupled to the ground state. Therefore, the cross section for collisional excitation is large and a significant percentage of the available copper atoms will be excited into these levels.

The resonance radiation will, at lower copper densities, quickly deplete this excitation before an inversion can be established. However, with sufficient copper vapor density the resonance transitions are radiatively trapped. This is equivalent to a lengthening of the natural lifetime of the resonance lines and changes the branching ratio to favor the (laser) transitions into the 4^2D levels. Thus, a population inversion of the 4^2P states relative to the 4^2D states can be obtained. Laser oscillation in the 510.5 nm and 578.2 nm lines results when optical feedback from mirrors is provided.

Quenching of the lower laser state is needed before the next discharge pulse can successfully produce an inversion. Under some conditions wall collisions are necessary[3] but collisions of the second kind with cool electrons can be effective with times as short as 14 microseconds[4,5]. Since this mechanism as well as the excitation mechanism is volumetric, laser output can be scaled by increasing the laser diameter.[6]

There is a complex interdependence of repetition rate with other parameters which dictates that this scaling might best be done at low repetition rates. The gas temperature in the center of a large tube operated at high repetition rates would be expected to become so high that thermal population of the lower laser state could result, limiting output.[7] Consequently, operation with interpulse periods long enough to allow gas cooling is desirable.

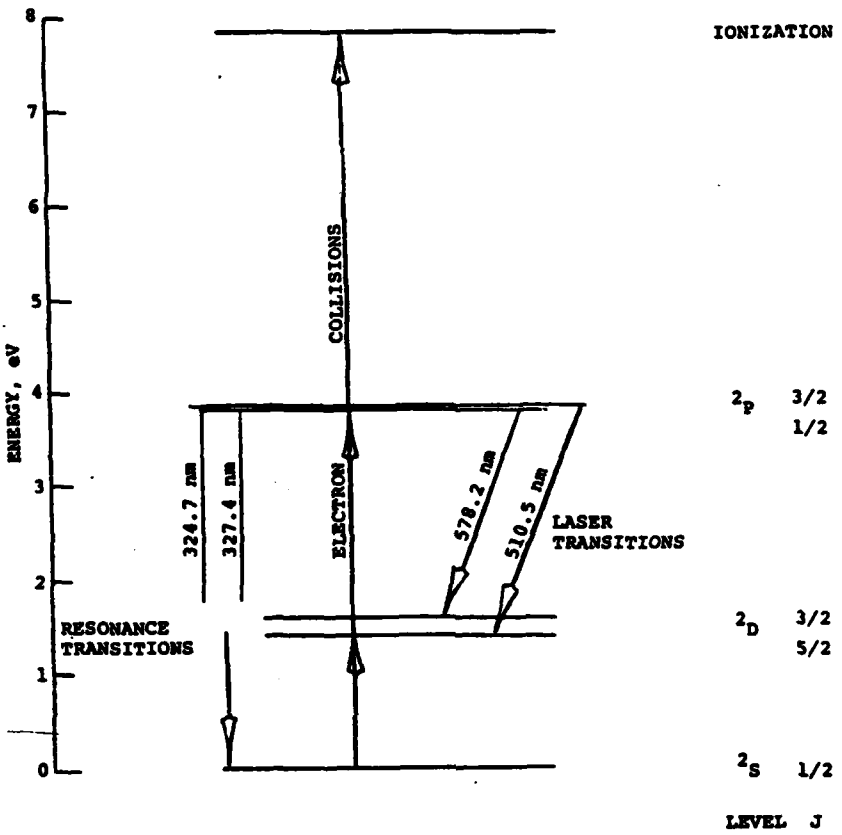

Figure 1. Simplified Copper Atom Energy Level Diagram

Long interpulse periods also allow time for recombination to proceed, decreasing plasma conductivity before and during breakdown. Reduced conductivity will, of course, lead to increased plasma resistance, a useful characteristic for large diameter lasers. The increased area of a large bore tube might otherwise produce such a low discharge resistance that high voltage drops cannot be sustained. This would limit laser output.[8]

Lowered conductivity could also reduce the effect of plasma shielding (i.e. skin effect). There is some concern that the combined effect of large discharge tube diameter and high plasma conductivity would prevent the electric fields, which heat the electrons, from penetrating to the tube axis. This effect has recently been investigated by Kushner for high repetition rate lasers (i.e. 5 KHZ) and found to be of concern for laser diameters of 8 cm and above.[9]

Finally, the lower level of electron density before each discharge pulse, resulting from lower repetition rate operation, should allow higher voltages to be used. It takes a higher voltage to bring the electron density up to a given density in a given time. Furthermore, higher electron temperatures will be produced improving upper laser state pumping and increasing the electron (and copper) densities that can be used.[10]

Consequently, in an attempt to dramatically increase the pulse energy produced by a copper vapor laser one would best direct attention not only to large volumes *but low repetition* rates, high voltages, and increased copper densities.

III. DEVELOPMENT AND VALIDATION OF THE COPPER VAPOR LASER COMPUTER SIMULATION MODEL

A. DESCRIPTION

Several years ago a copper laser computer model (CULSODE) was developed by M. J. Kushner and reported on in the literature.[10] An early form of this model using helium buffer gas was installed on the GE-SSD VAX computer in January 1981.

This program has advantages over earlier models in that it considers the afterglow period as well as the discharge period. Consequently, the preionization available before each repetitive pulse can be arrived at naturally. A stiff integrator that could handle the large variation in time steps, LSODE developed by A. Hindmarsh of Lawrence Livermore National Laboratory (LLNL), was also installed on the GE-SSD VAX.

CULSODE includes the following species and states:

a) Helium ground state, metastable state, and one higher excited state

b) Copper ground state, both metastable (lower laser) states, both resonance (upper laser) states, and one higher excited state.

c) Helium and copper ions.

d) Electrons

The particulate and radiative processes incorporated into the original program include electron impact phenomena (ionization, excitation, excitation relaxation, momentum transfer and radiative recombination); atomic collision effects (penning ionization, charge exchange and collisional relaxation); and of course radiative effects (spontaneous emission, stimulated emission and absorption). Radiative trapping is included as well as the effects of ambipolar diffusion of species and thermal conductivity to the walls.

B) COMPARISON OF CULSODE WITH EXPERIMENT

The earliest runs at GE describing copper laser output were essentially identical to those run by Kushner. In fact, some of his outputs[10], which were verified using the GE-SSD version of his code, agreed very well with the GE-SSD Model 6-15 Copper Laser data[11,12] (see Figure 2).

Comparisons were also made with output data obtained with 1.5 inch bore copper lasers at low repetition rates. Table 1 shows the laser characteristics and excellent agreement of the CULSODE prediction with measured output power. With appropriate choice of the initial electron density and other variables, the output after one iteration (i.e. pulse) was within a percent of that found after three iterations.

It should be noted that this agreement was obtained despite the lack of any inductance in CULSODE (see Figure 3). This, of course, led to pulse widths smaller than the experiment showed (see Table 1). In the case of the 1.5 inch bore laser at 1.0 kHz, this difference is a factor of two.

The lack of an inductor in the CULSODE model discharge circuit also led to the discharge capacitor maximum voltage being almost identical to that across the laser. It has been found that CULSQDE will accurately predict laser output when the voltage across the laser at "breakdown" (i.e. when discharge current begins to flow) is properly simulated. Unfortunately, for the computer model to simulate this the initial voltage drop across the capacitor must be significantly lower than that actually applied during experiment. Clearly, a substantial improvement in the computer model circuit was needed.

It should be noted here that since working at LLNL Kushner has also substantially improved his program. In fact he has gone another step in complexity by simulating radial distributions within the laser.[9,11] His intent was to determine radial effects in large bore high repetition rate high average power copper lasers. Consequently his results are of interest here and will be referred to later.

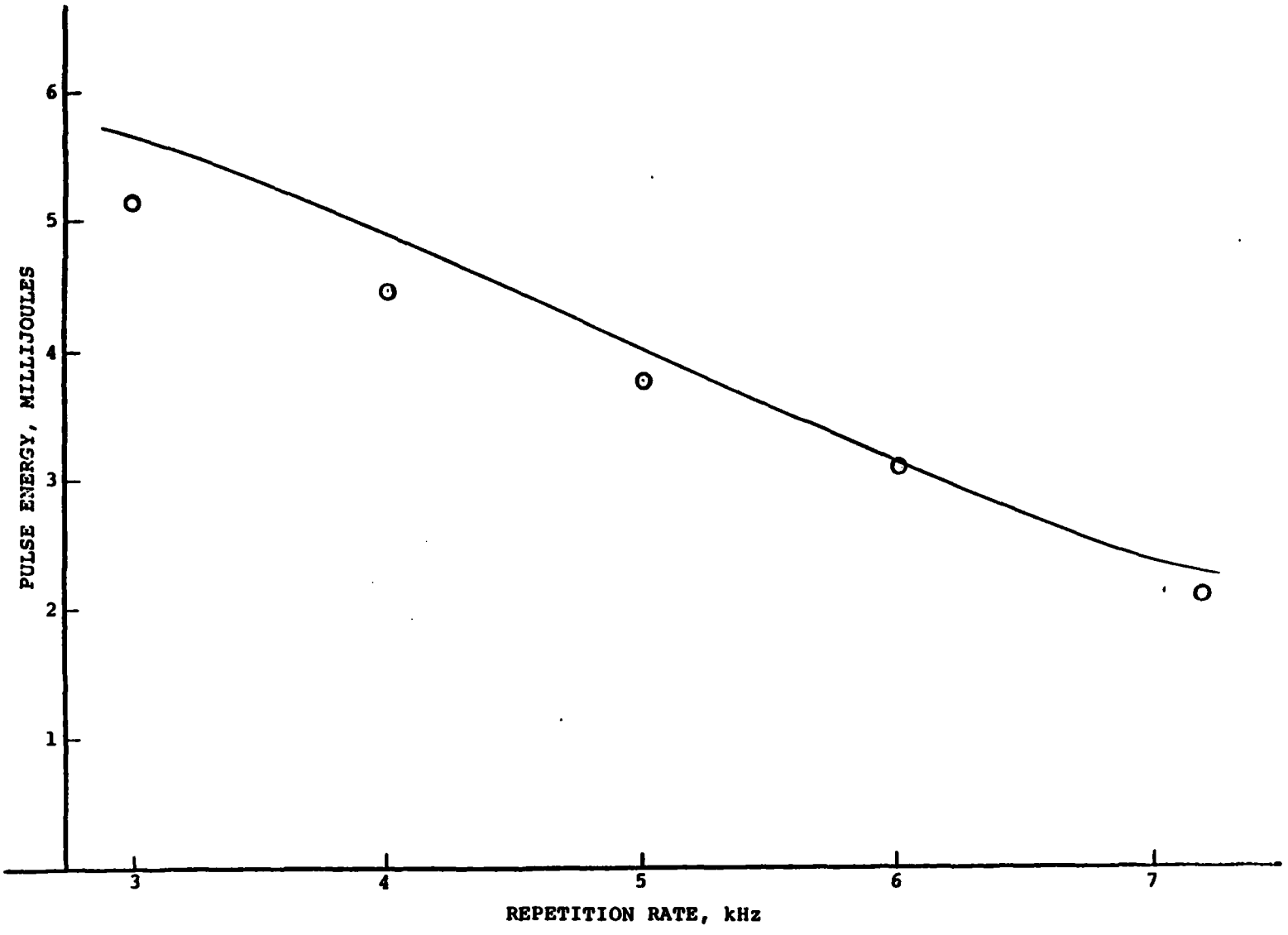

FIGURE 2. COMPUTER PREDICTIONS OF PULSE ENERGY AS FUNCTION OF REPETITION RATE AND EXPERIMENTAL DATA CORRELATING WITH IT.

TABLE 1

CHARACTERISTICS OF LASER USED FOR
COMPARISON OF CULSODE WITH EXPERIMENT

INPUT PARAMETERS

Tube Diameter:	1.5 inches
Capacitance:	20 x 10^{-9} farads
Interelectrode Length:	103 cm
Hot Zone Length:	64 cm
Temperature:	1700^{o}K
Helium Buffer Gas Pressure:	8 torr
Repetition Rate:	1 kHz
Voltage Across Laser:	13.5 kV

RESULTS

	CULSODE	EXPERIMENT
Output Power:	10.7 W	11.0 W
Pulse Width (FWHM):	20 nsec	40 nsec

C. COMPUTER MODEL MODIFICATIONS

The original CULSODE circuit (see Figure 3) has been replaced with a more realistic one (see Figure 4). This circuit includes not only the peaking capacitor C_p and parallel leakage resistor R_p but also the unavoidable parasitic inductances L_{s1} and L_{s2}. Furthermore, the thyratron switching function V_t was changed from the original relatively simple two-step voltage function to a three-stage function which includes a time dependent, switch closing reistance and a slow switch opening effect to simulate circuit recharge.

This circuit is solved by the current loop method. The current loop together with all the original chemical and radiative equations iterate to a final solution at each point in time before proceeding to the next time interval. The modified code is called CUHE 1.

Additional improvements have been incorporated into CUHE 1 and also into CUNE 1, a code developed for neon buffer gas operation.

a) The calculation of thermal transfer (gas heat loss to the walls) has been expanded so as to make it a function only of the buffer gas and other fundamental inputs. This replaces the previous simpler but semi-empirical heat transfer function and transfer input constant.

b) An option has been added to the program to permit automatic insurance of chemical balance/thermal balance for the first iteration's set of species. These initial species concentrations are internally calculated from pressure, gas and wall temperatures, and electron density.

c) A convenient plot routine has been added to allow rapid scanning and to provide hard copies of the results of selected output parameters.

d) The printout has been modified to include more input information, as well as some additional electrical and plasma characteristics in the output.

e) The code has been modified to change species concentration with changing gas temperature when proceeding from one laser pulse to the next.

f) Multiple cases, i.e. different input parameters, can now be set up in advance with far more case-to-case parameter variation than in CULSODE.

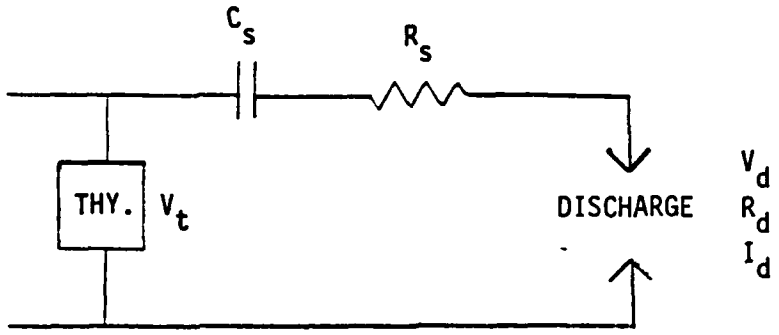

Figure 3. Electrical Circuit for CULSODE. Voltage across the thyratron is V_t, while C_s and R_s are series capacitor and resistor, respectively. Sub-d refers to discharge parameters.

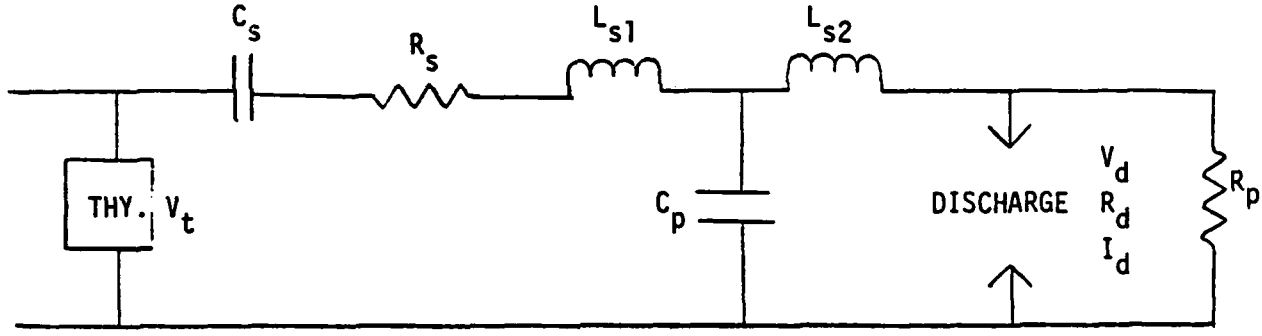

Figure 4. Electrical Circuit for CUHE 1 and CUNE 1. Series inductances are L_{s1} and L_{s2}, while Cp is the peaking capacitor and R_p is parallel resistance.

g) Perhaps most important, the parameters involving the helium buffer gas have been replaced with equivalent parameters involving neon to create a new code called CUNE 1. This required changing all appropriate atomic energy levels, rate constants, radiative lifetimes, atomic weights, and diffusion coefficients.

h) Caution must be exercised in extending code operation to diameters exceeding the skin depth, above 25 eV, and below 10^{10} electrons cm^{-3}. Inaccuracies will begin due to basic assumptions.

D. VALIDATION OF CUHE 1

Several different lasers were simulated by the CUHE 1 model. The major effort was directed toward the GE-SSD Model 6-15 Laser which has a 1.0 inch bore. This laser model has been used in various Air Force and LLNL programs and has been sold to other customers. The CUHE 1 simulations predicted average power of 12 to 20 watts under conditions that produced similar power experimentally. In general, the agreement with experiment obtained earlier with CULSODE was preserved with the addition that the time dependences were now properly reproduced (see Figure 5 and 6). Note that the voltage is measured at a point somewhere between the laser and the pulse sharpening capacitor and that detailed agreement with the green pulse amplitude and late time behavior are absent.

Increase of the laser bore to 1.5 inches and reduction of the repetition rate to 1.0 kHz, to match another well characterized laser, produced a similar agreement with predictions and measurements. Operating conditions that produced 12.1 mJ per pulse experimentally, were predicted to produce 13.6 mJ per pulse.

Table 2 lists the input characteristics. Table 3 lists the output characteristics showing the degree of agreement achieved. It is interesting to note that the laser pulse width was properly simulated in this case. In most high power operation, although the pulse energy and other characteristics are properly simulated, the complex pulse shape is not. The computer model generally predicts a smooth pulse with a single maximum but at high power the actual output often has an extended multimaximum form. Only when the output is smooth or the distortion is not large will the model properly simulate the pulse shape. Note that this is a common flaw and is even encountered with the LLNL two-dimensional copper laser model.[13]

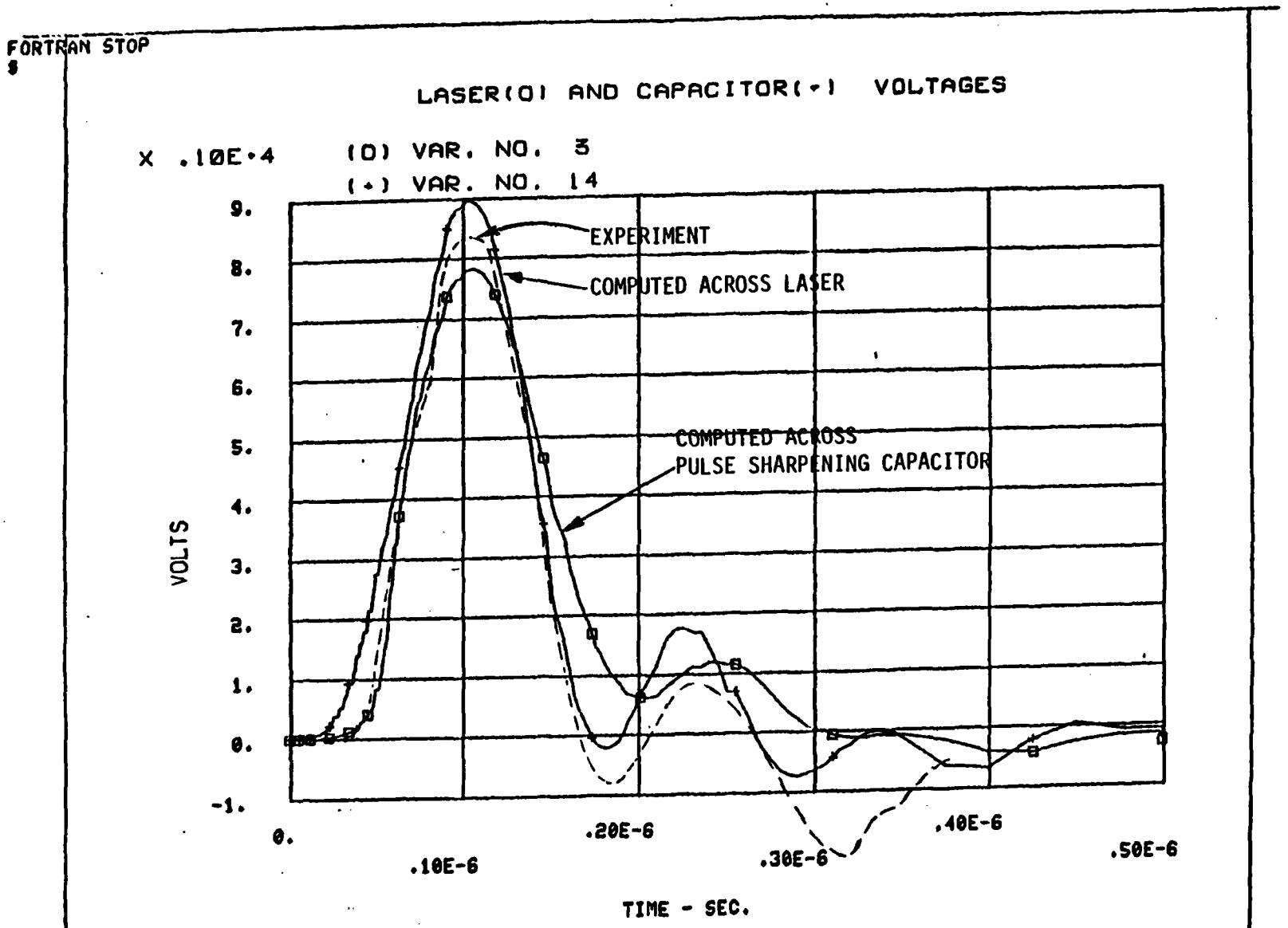

FIGURE 5

COMPARISON OF COMPUTED TIME RESOLVED VOLTAGE DROP WITH EXPERIMENT

FORTRAN STOP
0

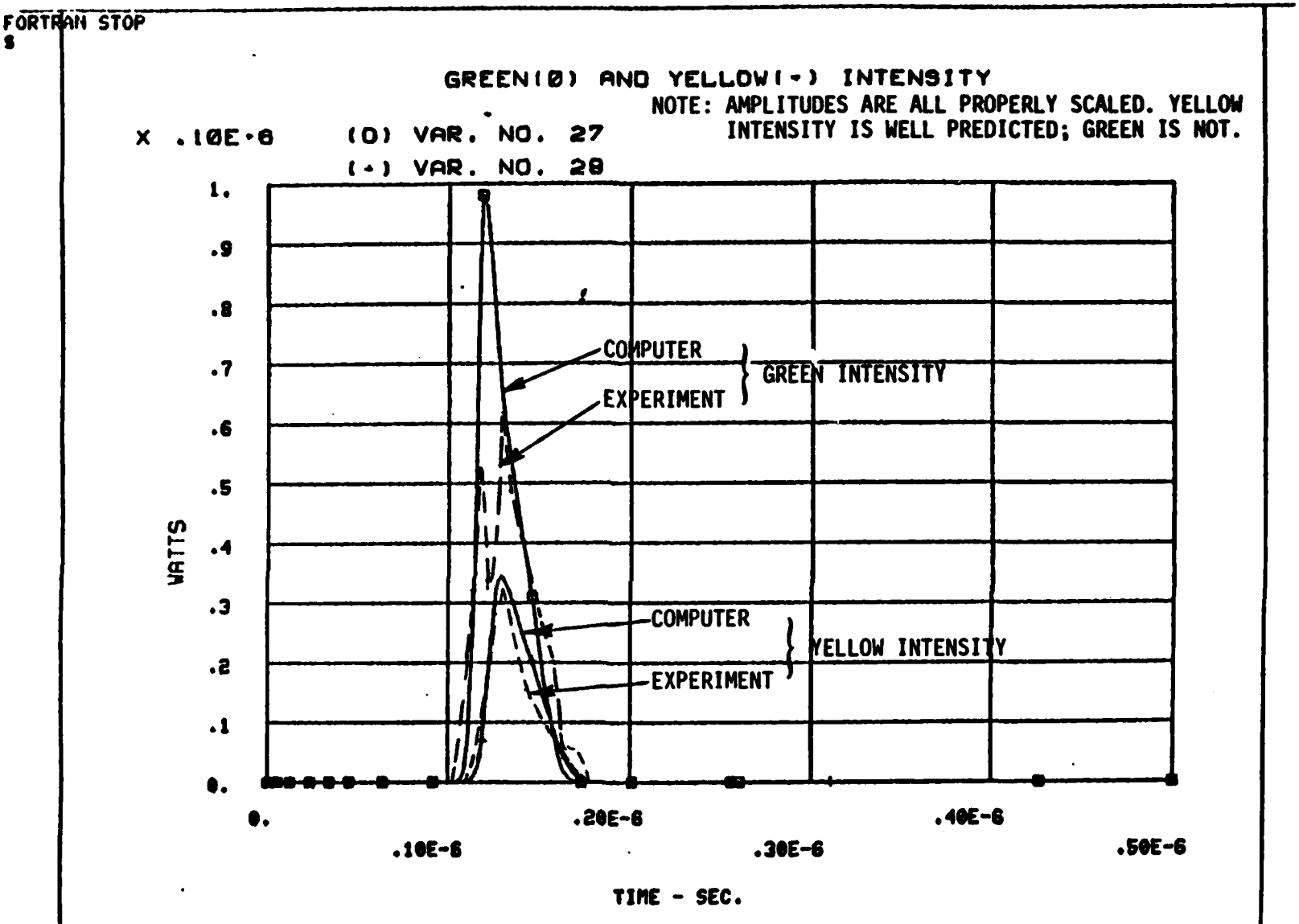

FIGURE 6

COMPARISON OF TIME RESOLVED LASER POWER WITH EXPERIMENT

TABLE 2.

INPUT CHARACTERISTICS OF 1.5 INCH BORE LASER

Discharge Tube Diameter:	3.8 cm
Discharge Length:	103 cm
Hot Zone Length:	64 cm
Optical Cavity Length:	185 cm
Initial Capacitor Voltage:	22 kV
Storage Capacitance:	20 nF
Peaking Capacitance:	9 nF
Thyratron Loop Inductance:	174 nH
Peaking Capacitor Loop Inductance:	200 nH
Long Term Circuit Resistance	0.01 ohm
Charging Resistor:	150 ohm
Initial Thyratron Resistance:	1×10^4 ohm
Switching Time Constant:	5 nsec
Equilibrium Copper Density:	$7.7 \times 10^{14}/cm^3$
Helium Pressure:	8 torr
Repetition Rate:	1 kHz

TABLE 3.

COMPARISON OF OUTPUT CHARACTERISTICS OF 1.5 INCH BORE LASER

	EXPERIMENT	CUHE 1
Pulse Energy:	12.1 mJ	13.6 mJ
Green/Yellow Ratio:	2.04	2.04
Pulse Width (FWHM):	45 nsec	45 nsec

E. VALIDATION OF CUNE 1

Large bore laser experiments conducted at LLNL have been used to validate the copper/neon code, CUNE 1. The most detailed comparison has been accomplished with data from a 6 cm bore laser built and tested by GE-SSD personnel under contract with LLNL[14]. More data and comparison with a LLNL computer model were presented at a later date.[13] Table 4 lists the laser input characteristics and Table 5 lists the output characteristics. The measured data and the CUNE 1 predictions can be seen to be in generally good agreement (as good as that obtained with the LLNL two-dimensional code).[13] Similar agreement is obtained for the discharge current as is shown in Figures 7 and 8. Figures 9 and 10 respectively show the simulated voltage drop across the laser plasma and across the peaking capacitor. Figure 11 shows the voltage drop measured at some intermediate position. Taking into consideration this uncertainty in exactly where the voltage was measured, as with CUHE 1 and Figure 5 the agreement is quite acceptable. Figures 12 to 14 are CUNE 1 generated graphs of other parameters of interest from the simulation of the 6 cm bore laser.

TABLE 4

INPUT CHARACTERISTICS OF 6 CM BORE LASER EXPERIMENT

Discharge Tube Diameter:	6 cm
Discharge Length:	122 cm
Hot Zone Length:	102 cm
Optical Cavity Length:	250 cm
Initial Capacitor Voltage:	18 kV
Storage Capacitance:	12 nF
Peaking Capacitance:	4 nF
Thyratron Loop Inductance:	275 nH
Peaking Capacitor Loop Inductance:	350 nH
Long Term Circuit Resistance:	2 ohm
Charging Resistor:	200 ohm
Initial Thyratron Resistance:	10^4 ohm
Switching Time Constant:	5 nsec
Beginning of Charge Cycle:	0.1 msec
End of Charge Cycle:	0.2 msec
Copper Density:	$1.1 \times 10^{15}/cm^3$
Neon Pressure:	60 torr
Repetition Rate:	5 kHz

TABLE 5.

COMPARISON OF OUTPUT CHARACTERISTICS OF A 6 CM BORE LASER

	COMPUTER MODEL (CUNE 1)	EXPERIMENT
Total Output Power:	66 watts	60 watts
Green Output Power:	49 watts	43 watts
Maximum Upper State Pop. Density:	4.3×10^{12} cm^{-3}	6.0×10^{12} cm^{-3}
Maximum Lower State Pop. Density:	1.0×10^{14} cm^{-3}	8.0×10^{13} cm^{-3}
Minimum Lower State Pop. Density: (Afterglow)	2.2×10^{12} cm^{-3}	3.0×10^{12} cm^{-3}
Electron Density in Afterglow:	3.1×10^{13} cm^{-3}	3.0×10^{13} cm^{-3}

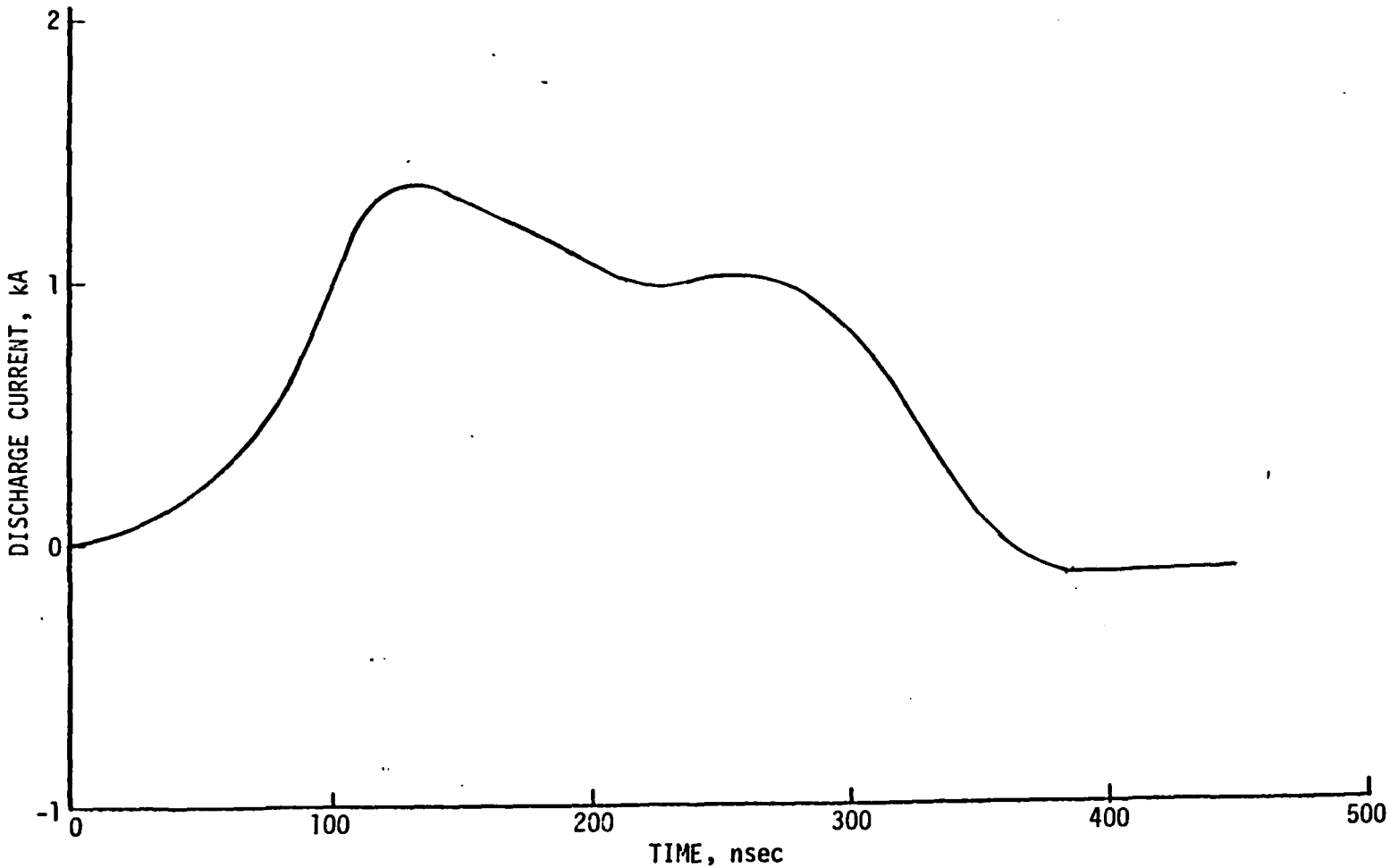

Figure 7. Measured Discharge Current in 6 cm Diameter Laser

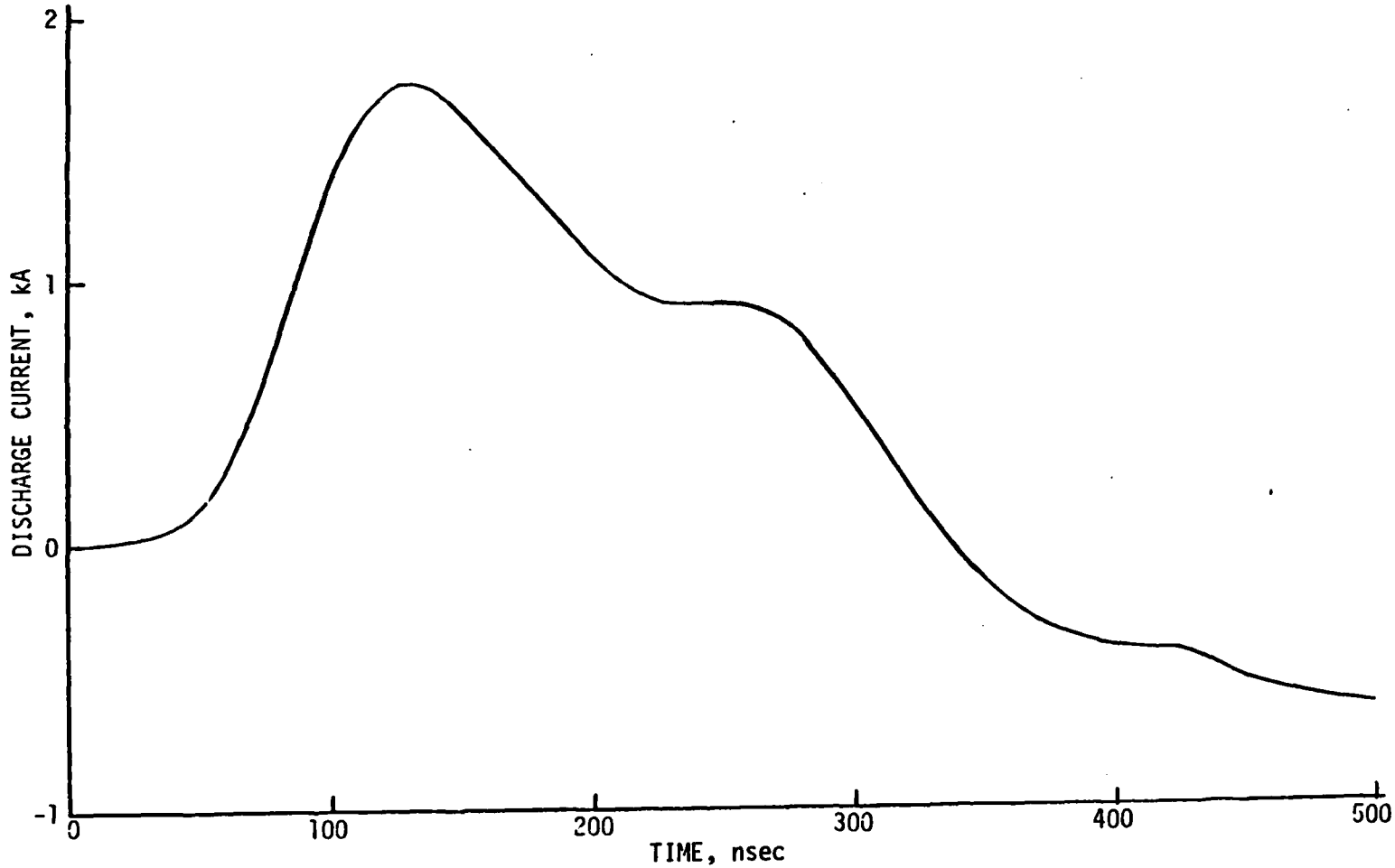

Figure 8. Discharge Current in 6 cm Diameter Laser. Simulated with CUNE 1 Computer Model.

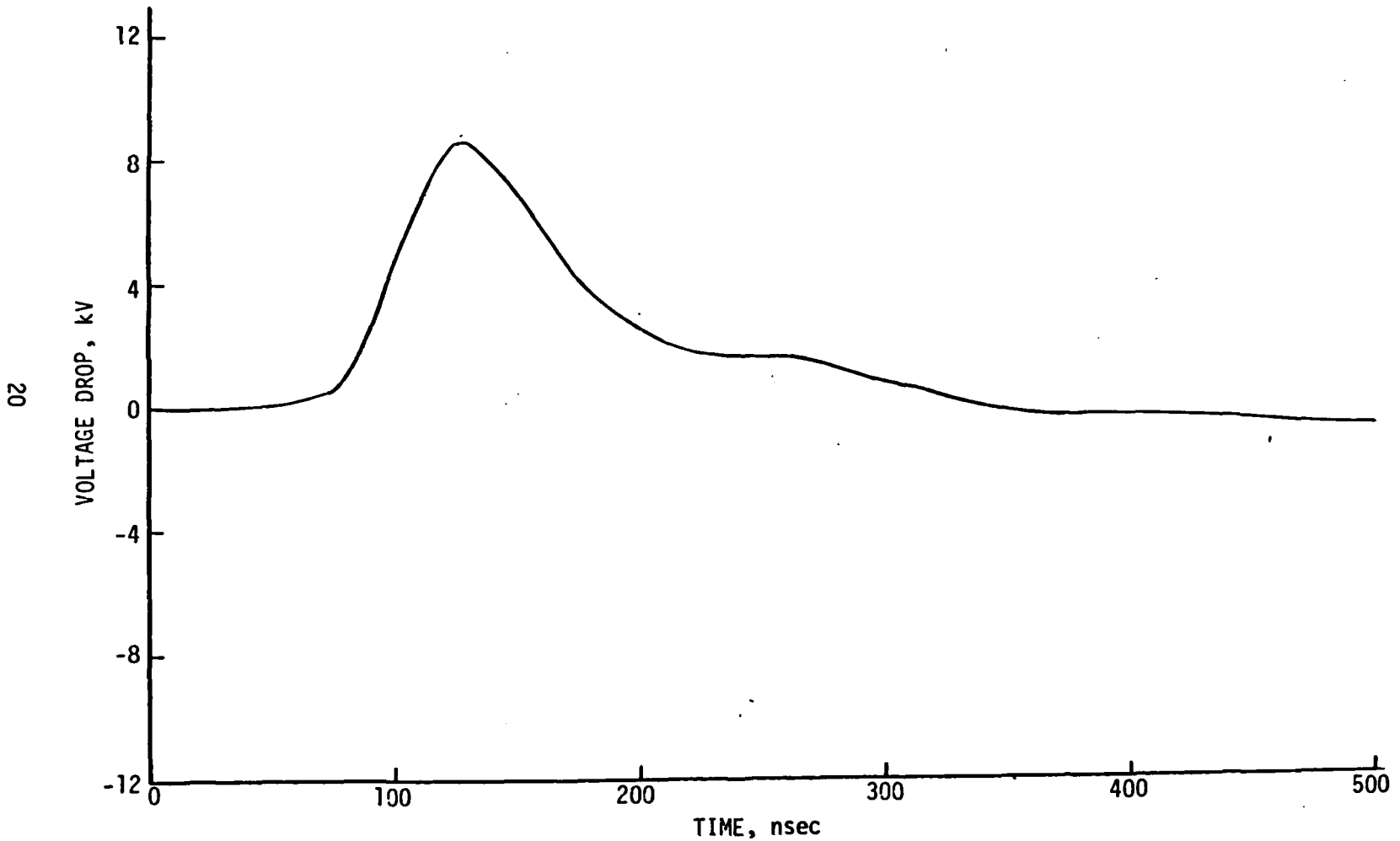

Figure 9. Voltage Drop Across 6 cm Diameter Laser. Simulated with CUNE 1 Computer Model.

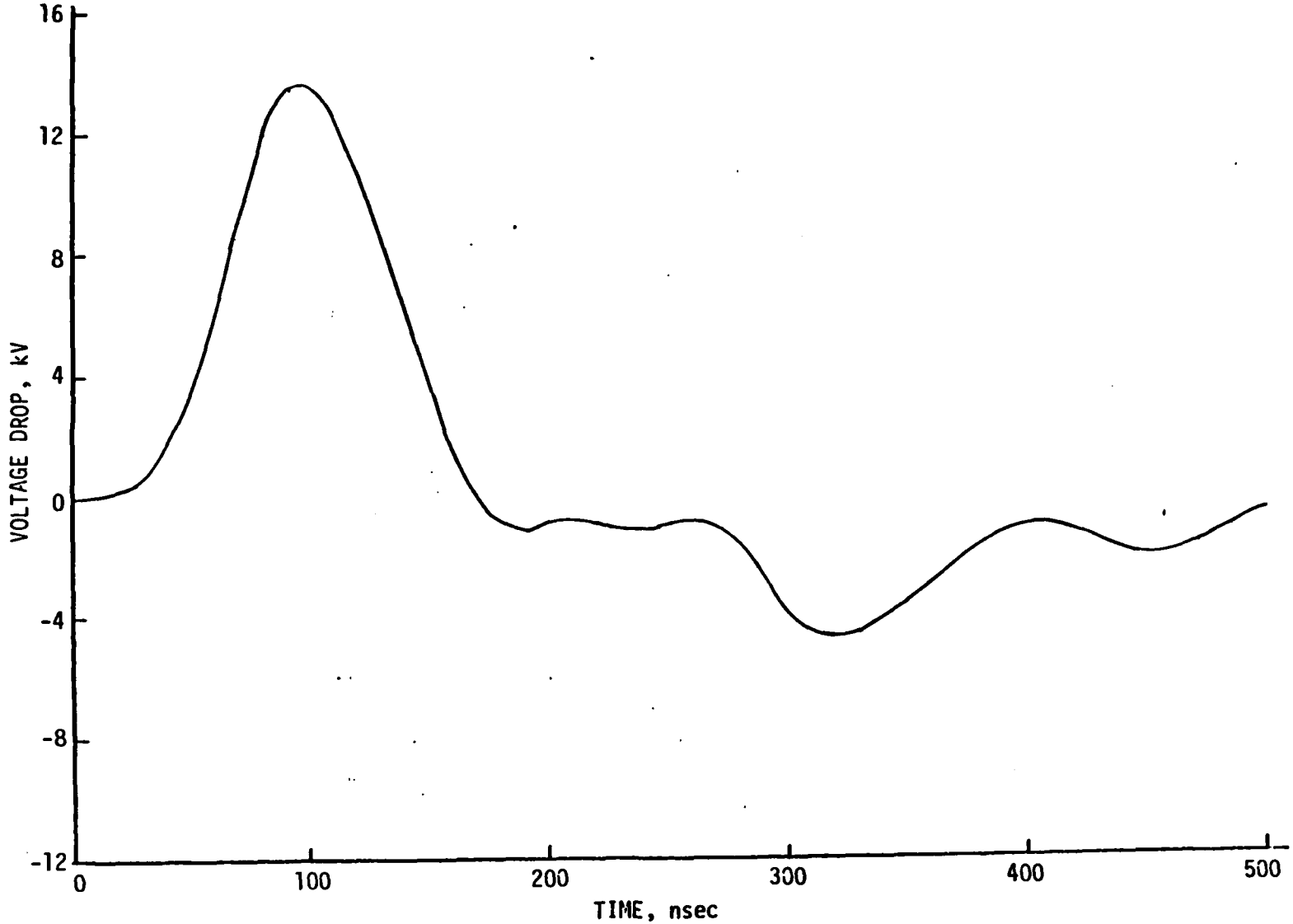

Figure 10. Voltage Drop Across Peaking Capacitor of 6 cm Diameter Laser. Simulated with CUNE 1 Computer Model.

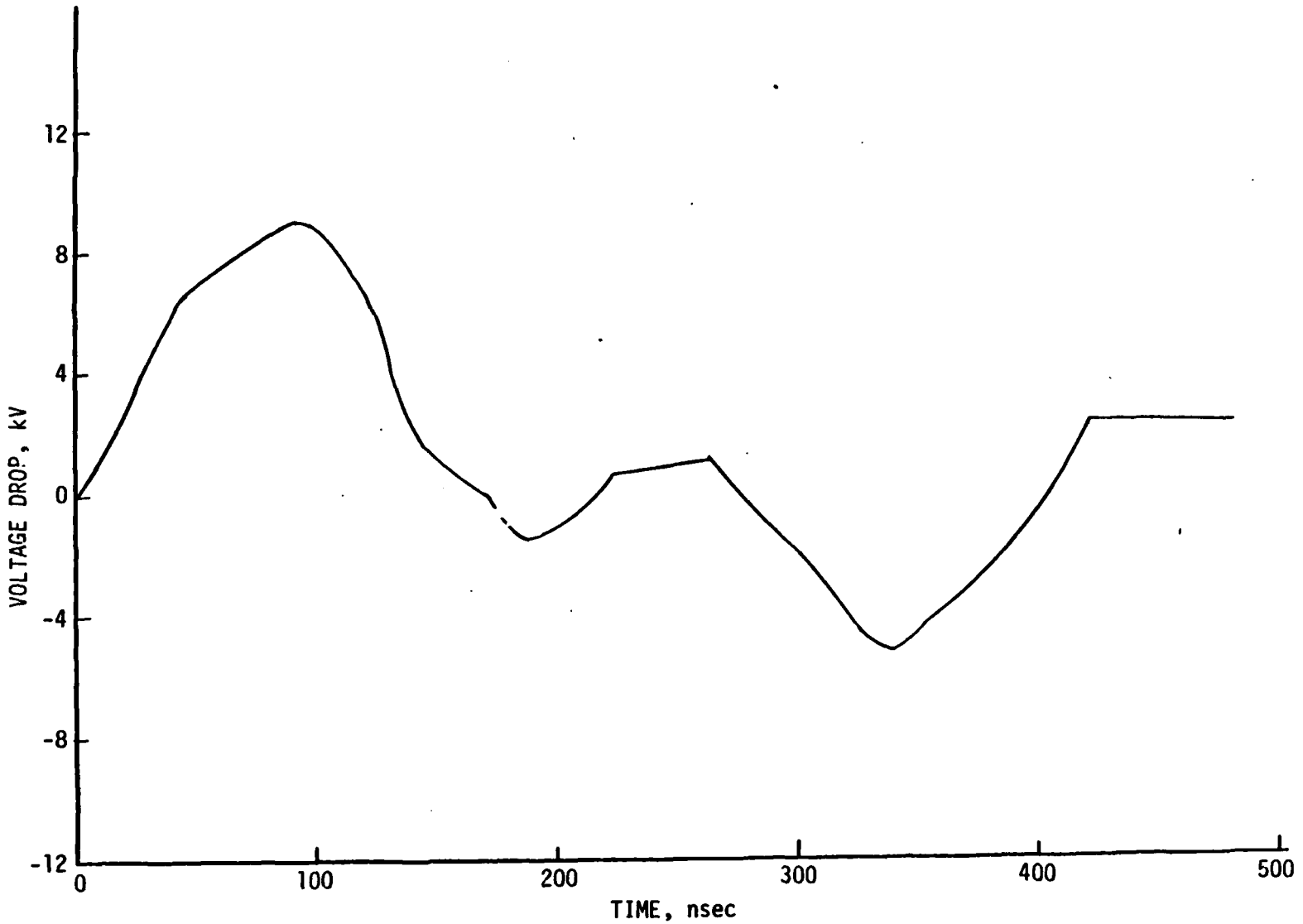

Figure 11. Measured Voltage Drop of 6 cm Diameter Laser

17

FIGURE 12.

ELECTRON TEMPERATURE SIMULATED FOR 6 cm DIAMETER LASER

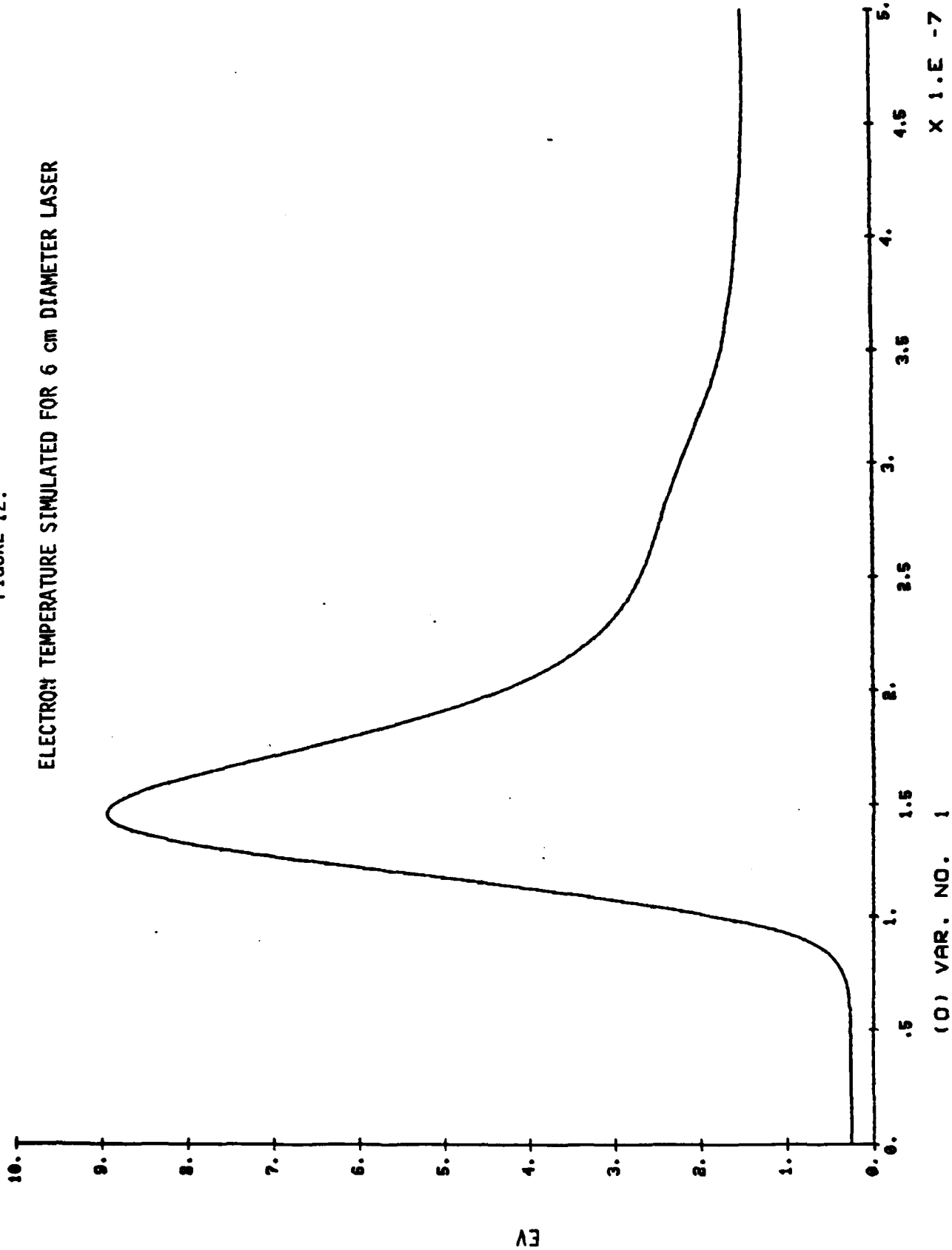

FIGURE 13.

ELECTRONIC DENSITY SIMULATED FOR 6 cm DIAMETER LASER

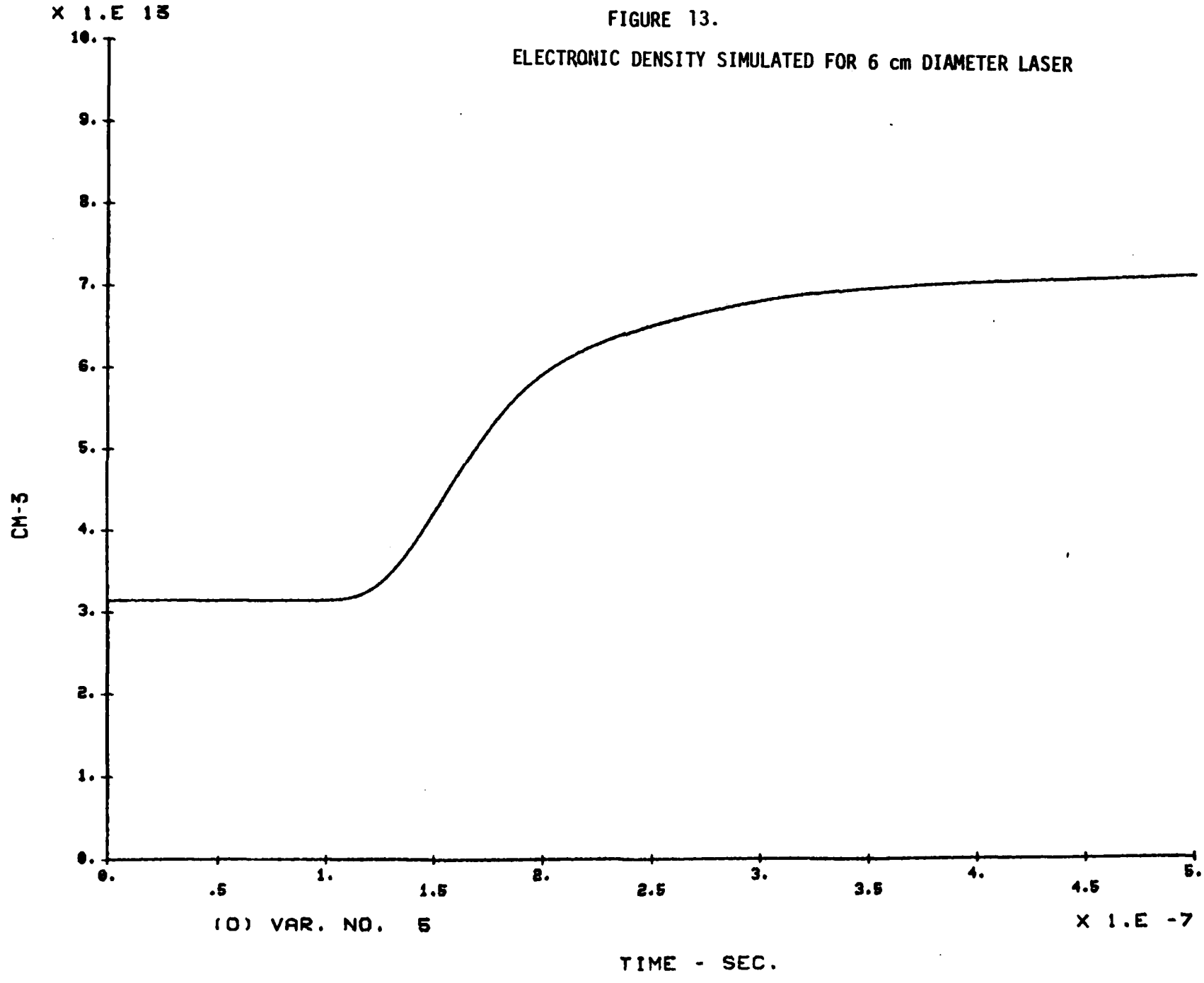

FIGURE 14. PULSE ENERGY SIMULATED FOR 6 cm DIAMETER LASER

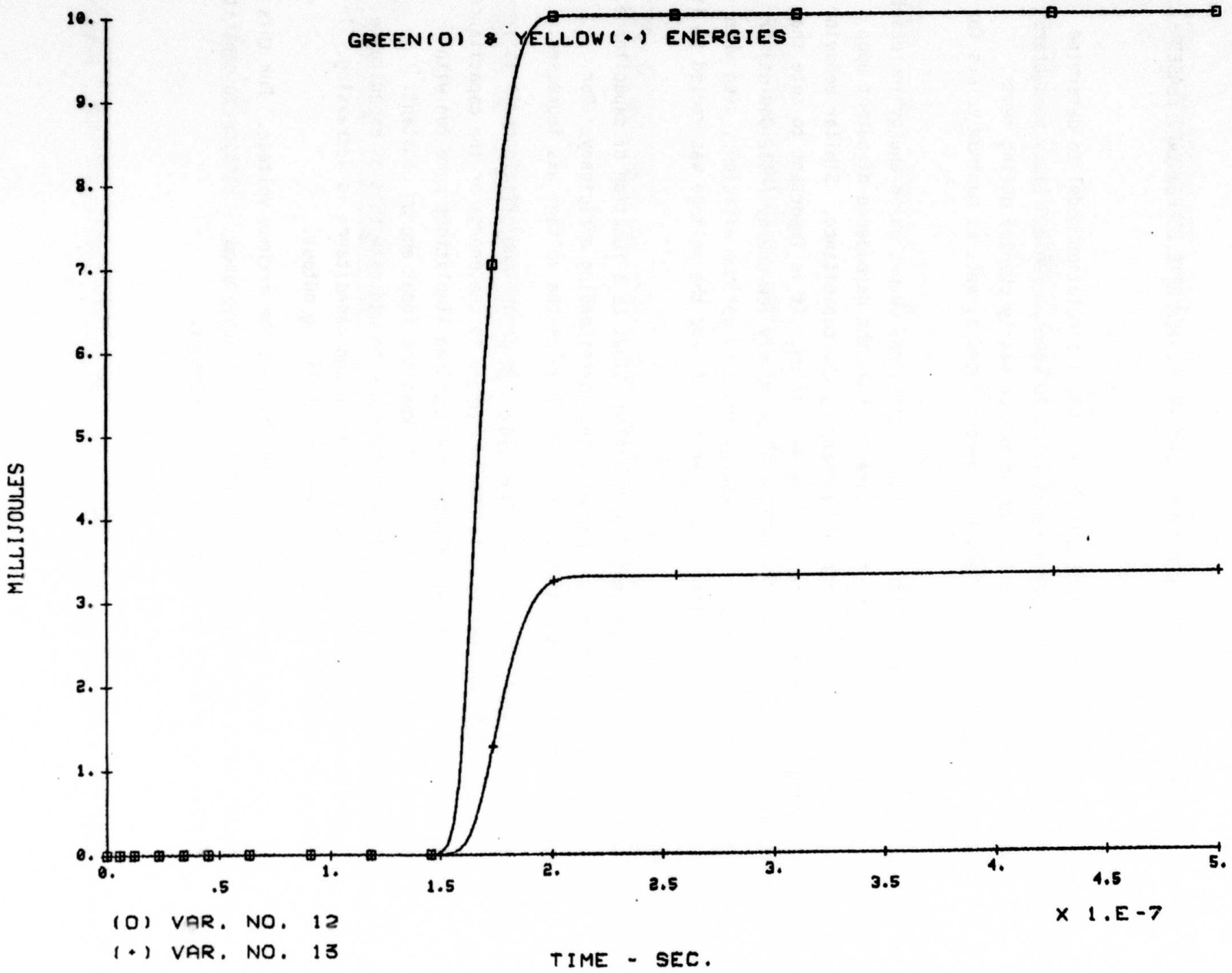

IV. SIMULATION OF A 10 CM DIAMETER LOW REPETITION RATE COPPER VAPOR LASER

A. DISCUSSION

An investigation was conducted with the CUNE 1 simulation model to determine optimum input characteristics for a 10 cm ID laser. Table 6 lists parameters that were not varied since they could not be easily changed during tests. Table 7 lists those parameters that were changed as well as maximum values for those parameters.

As indicated by the earlier empirical studies the output pulse energy increased with electrical energy input. Figure 15 shows the dependence of output upon input when the input was varied by changing the capacitance. Similar behavior was found when the capacitor voltage was varied. It is important to note that a maximum efficiency was reached for a moderately low energy ($\sim$12 Joules) or 1 mJ/cm^3 specific energy). This energy produced optimum efficiency even when a higher value of capacitance was used (19 nf) and the voltage was varied to its optimum (32 kV).

The same data can be presented by plotting output as a function of capacitance. This is shown on Figure 16 along with the corresponding efficiency. For reference a similar set of data is shown in which the voltage was increased.

While it is clear from this data that there is an optimum efficiency it is uncertain as to whether this is due to changes in the energy or the capacitance (voltage). In order to illuminate this question simulations were run with capacitance and voltage varied so as to keep the input energy constant. Figures 17 and 18 show the voltage dependence to dominate that of capacitance. Increasing voltage increases output even though capacitance is decreasing. In contrast increasing capacitance leads to declining output.

The highest output and efficiency were found at the maximum voltage. For this reason Figure 16 and other simulations of this group used 60 kV storage capacitor voltage, the highest contemplated for experiments.

TABLE 6

PARAMETERS FIXED BY EXPERIMENT DESIGN

Laser Tube Diameter	10 cm
Discharge Length	178 cm
Optical Cavity Length	250 cm
Hot Zone Length	150 cm
Thyratron Switching Time Constant	5 ns
Output Mirror Reflectivity	.08
Charging Resistor	200 Ω

TABLE 7

PARAMETERS VARIED

Parameter	Maximum Value
Neon Buffer Pressure (P)	60 torr
Copper Vapor Density (NC)	1.2×10^{15} cm^{-3}
Voltage (V)	50 KV
Storage Capacitance (Ca)	51 nf
Thyratron Loop Inductance (L_1)	500 nh
Repetition Rate (R)	200 hZ
Discharge Loop Inductance (L_2)	450 nh
Peaking Capacitor (CP)	19 nf

Figure 15. Variation of Output Pulse Energy at 510.5 nm and Efficiency as Function of Stored Energy Per Pulse.
Obtained by Varying Capacitance, Voltage Held Constant.

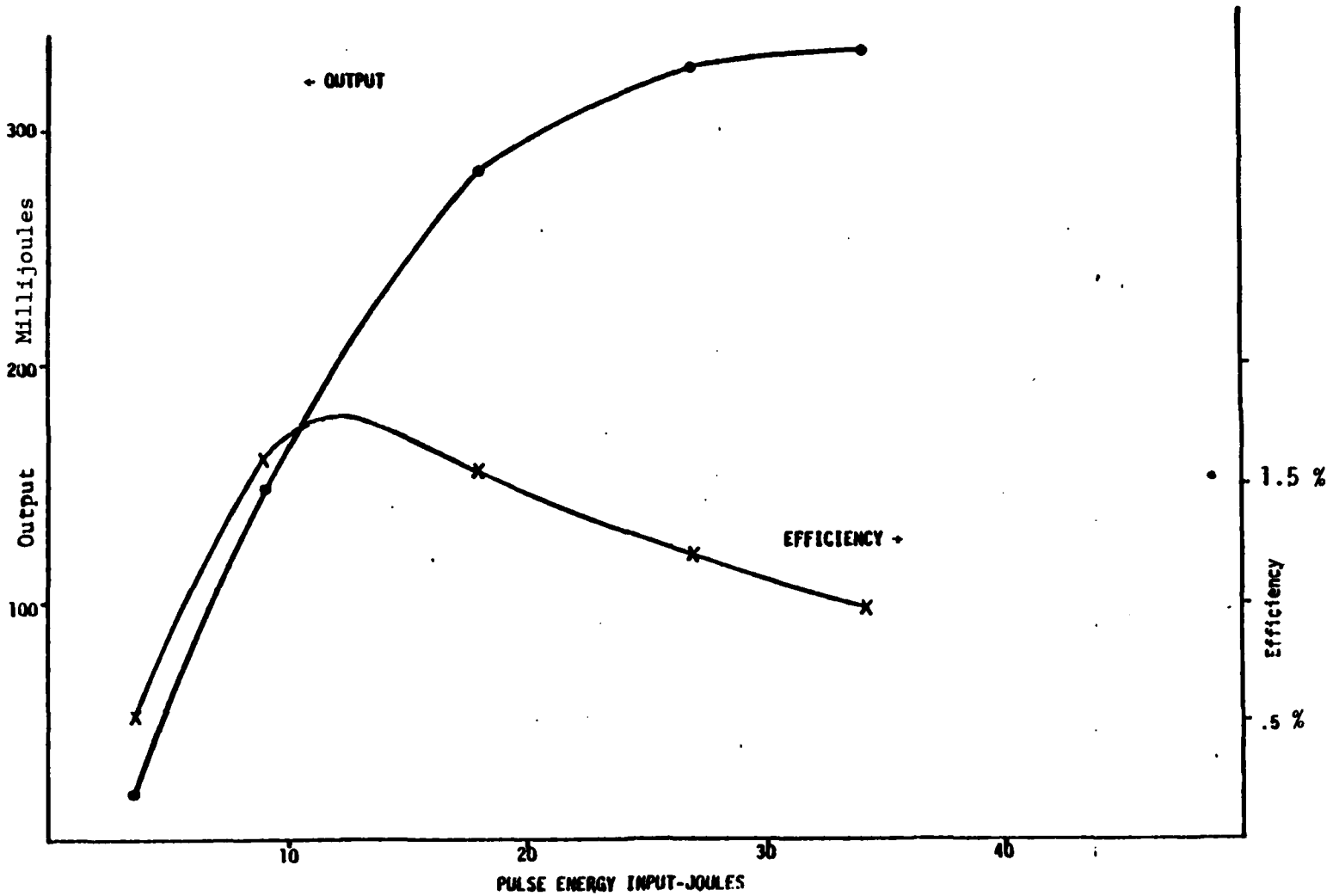

Figure 16. Variation of Output Pulse Energy at 510.5 nm and Efficiency as Function of Capacitance (constant voltage is 60 kv) and as Function of Voltage (Constant Capacitance is 19 nf).

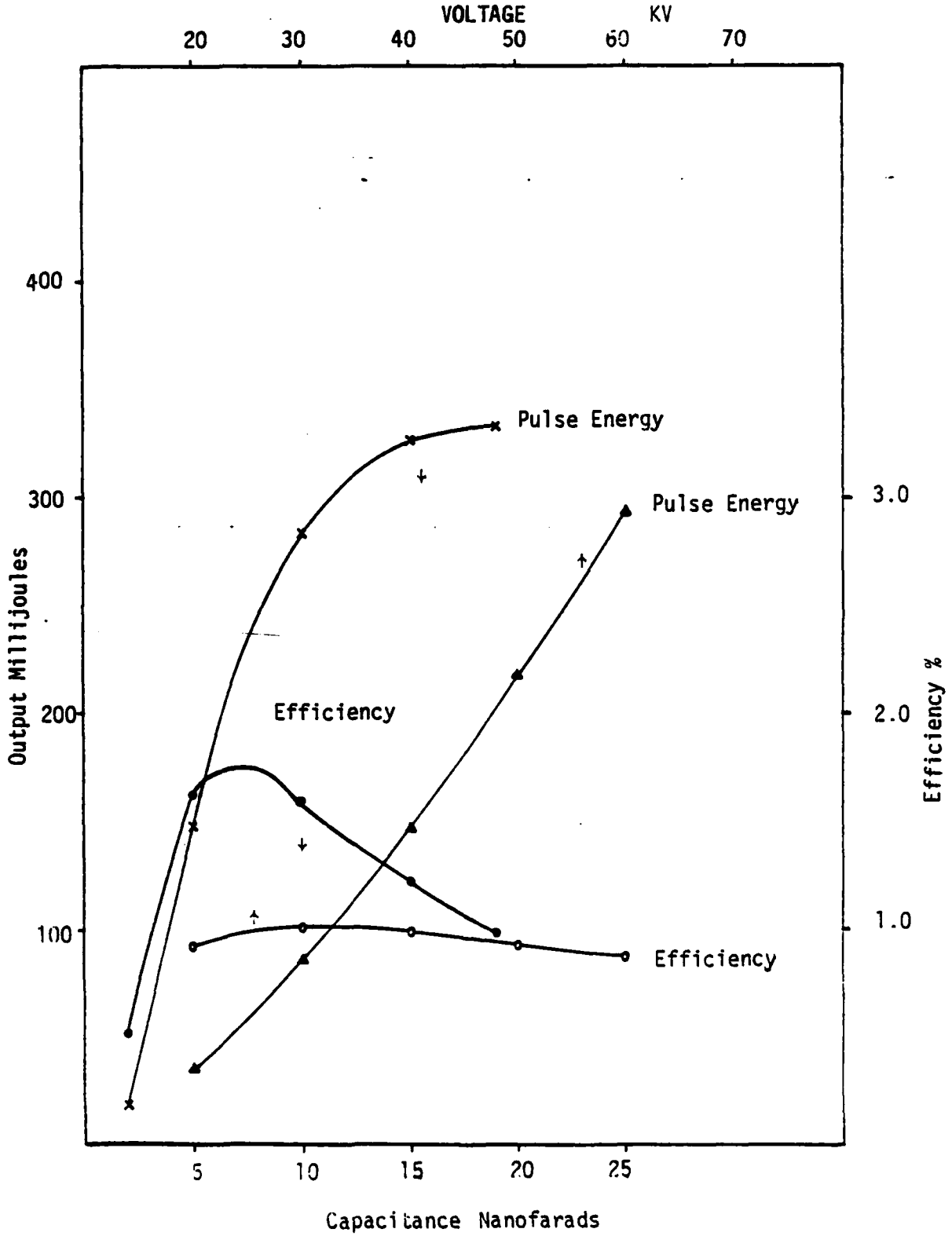

Figure 17. Output Pulse Energy as Function of Discharge Capacitance. Discharge Pulse Energy is Constant at 34 Joules. Obtained by Varying Capacitance and Voltage Simultaneously.
This Figure and Figure 18 Plot the same Information except the Variable used on the Absissa has changed.

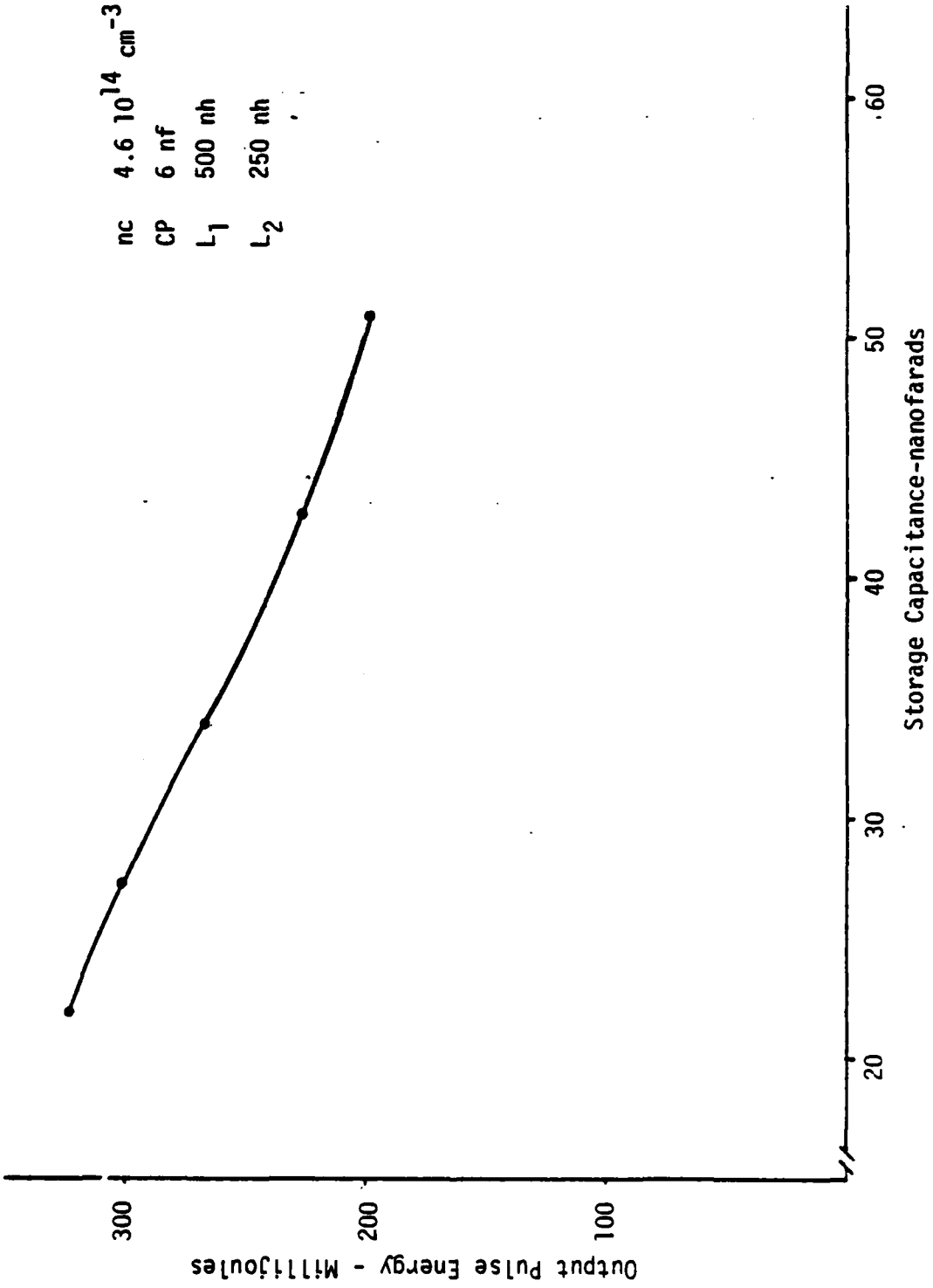

FIGURE 18. OUTPUT PULSE ENERGY AS FUNCTION OF STORAGE CAPACITOR VOLTAGE. SEE FIGURE 17.

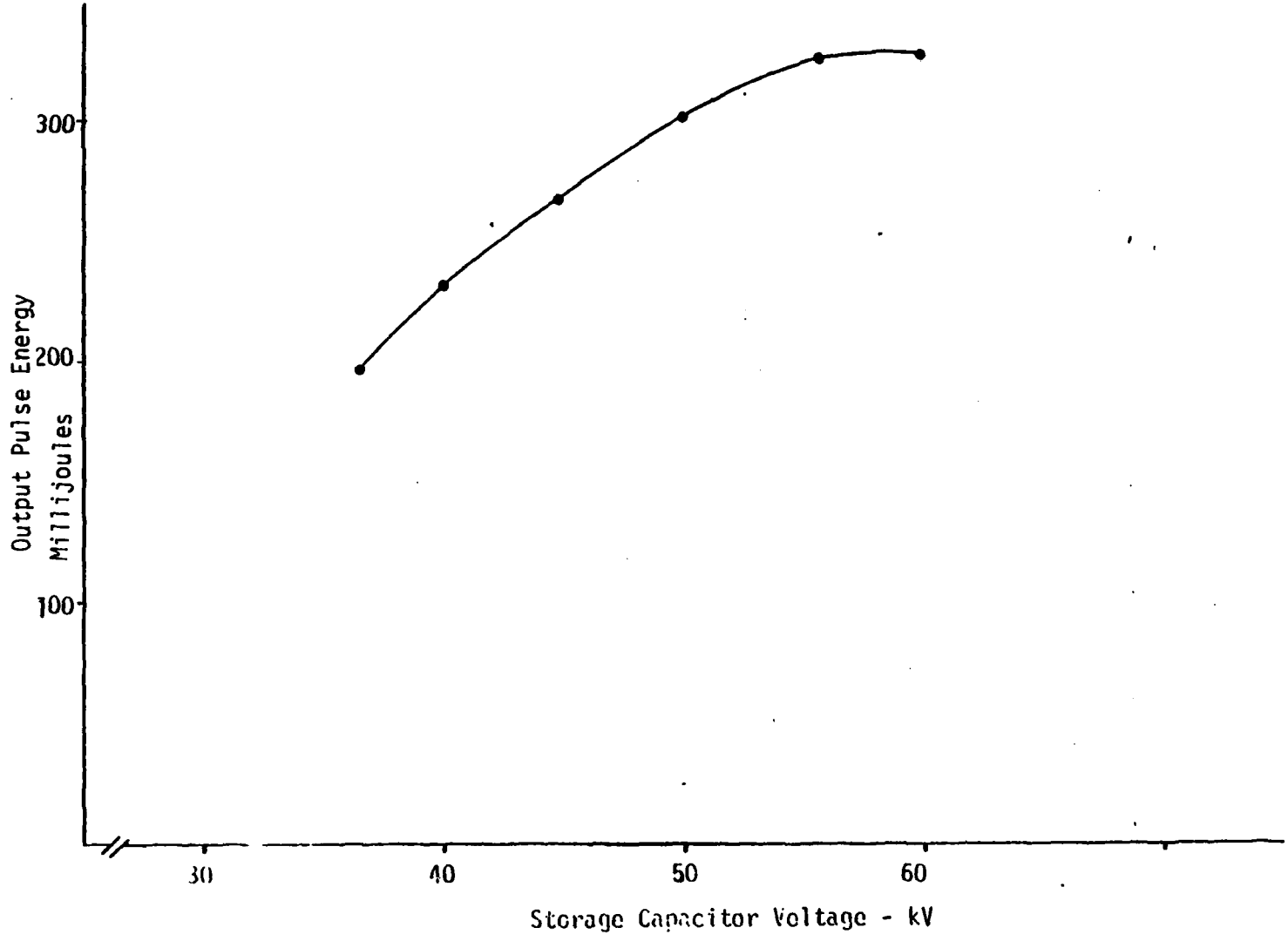

It should be noted here that the output and efficiency produced with 10 nf/5 nf capacitance and 60 kV (Figure 16) correspond very closely to the oscillator design point arrived at on empirical grounds earlier[1] (1.5 mJ/cm^3 specific loading, 24 μJ/cm^3 output, and 1.6% efficiency simulated vs 1.5 mJ/cm^3, 25 μJ/cm^3, 1.67% projected empirically). This agreement is quite significant because it represents support of computer model results at large diameter with experimentally derived data. Optimized 10 nf/2 nf result: gave .337 J at 1.8% efficiency.

Further analyses of the effect of varying capacitance can be seen on Figure 19. There the output is explored for three low values of the storage capacitance as a function of the pulse sharpening (or peaking) capacitance. It can be seen that the optimum shifts to lower values a the storage capacitance is reduced. Comparison of Figure 19 with Figure 17 shows the highest optimum is obtained with storage capacitance of about 19 nf, and pulse sharpening capacitance of 3-5 nf. Also note 5 nf capacitance yields 2.5% efficiency.

A similar variable is the inductance in that it can be approximated by two lumped values (Figure 20). The inductance of the inner loop (see Figure 4) contains the laser itself as well as the pulse sharpening capacitor. The outer loop inductance contains the thyratron switch and the main storage capacitor.

The dependence of the output pulse energy upon inductance value is shown on Figure 20 and 21 to be quite weak in the range covered. For some capacitance values change in outer loop inductance makes no difference at all (Figure 20). However, there is usually some optimization that is possible (Figure 21). For this reason the inner loop inductance is best kept as small as possible and the outer loop inductance somewhat larger.

In contrast, Figure 22 shows a large difference in the dependence of output on inner loop inductance when the storage capacitance is changed. The data here are for a 12 cm diameter laser and it can be seen that 19 nf is still optimum as is a minimum inductance.

The effect of changing the length of the active zone can be seen on Figure 23 and 24. The former shows that with a constant specific loading the output remains roughly constant. This is due to the fact that the field strength is

FIGURE 19. VARIATION OF PULSE ENERGY OUTPUT AT 510.5 nm WITH PULSE SHARPENING CAPACITANCE.
STORAGE CAPACITANCE IS CONSTANT.

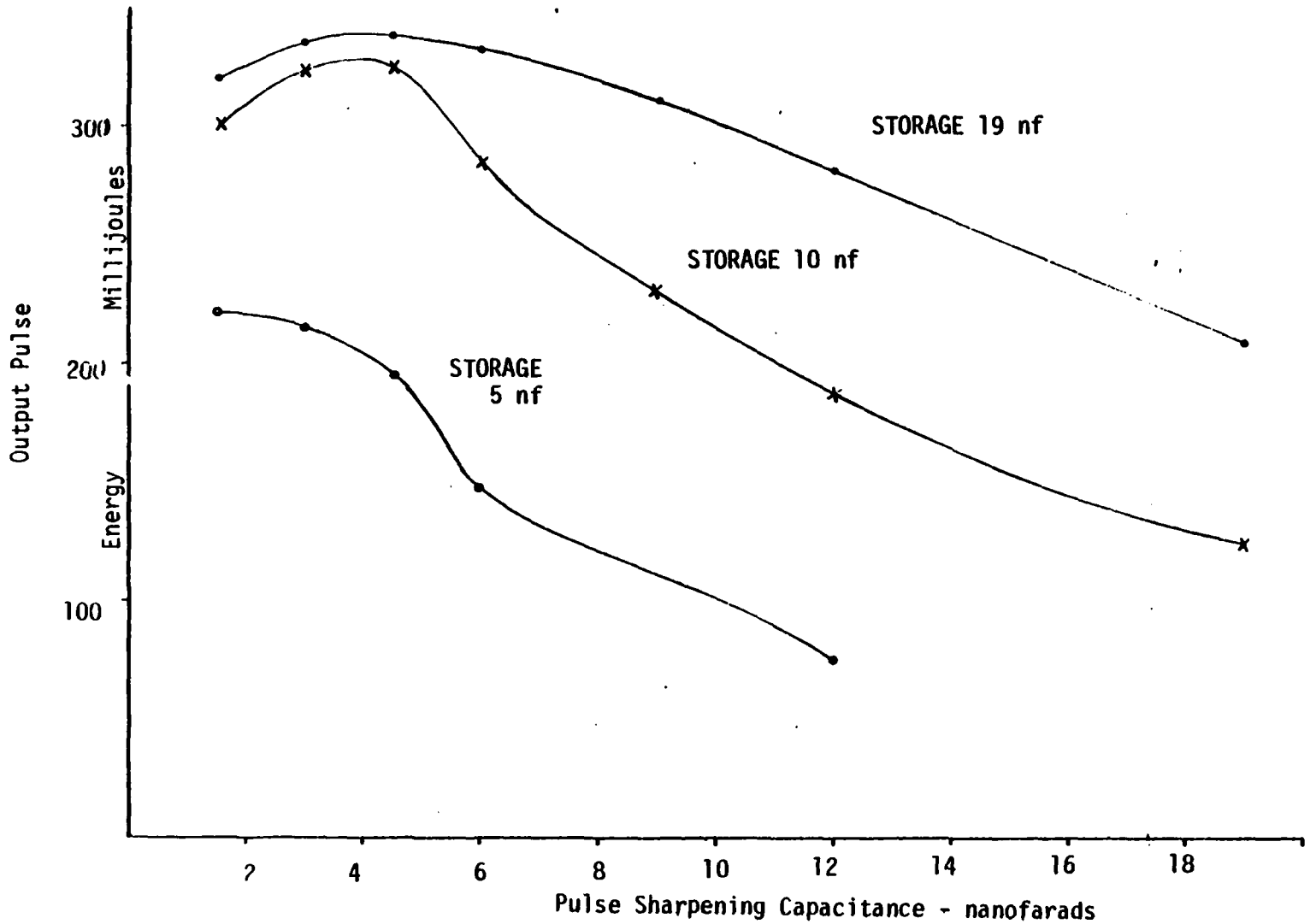

Figure 20. Variation of 510.5 nm Output with Inner Loop Inductance. Outer Loop Inductance is a Constant Parameter.

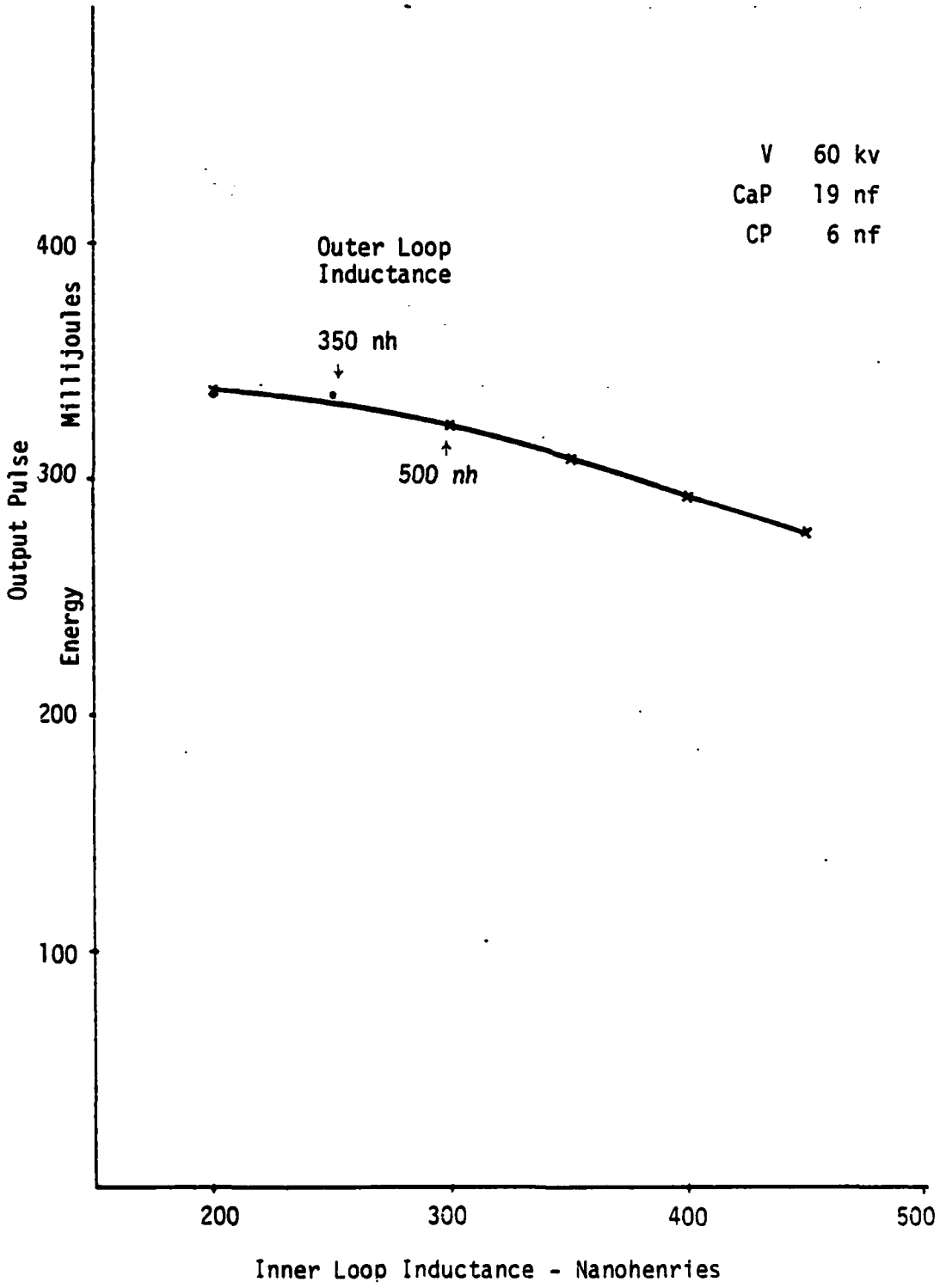

FIGURE 21. VARIATION OF OUTPUT AT 510.5 nm WITH INNER LOOP INDUCTANCE (L_2 ON FIGURE 4). OUTER LOOP INDUCTANCE IS A PARAMETER.

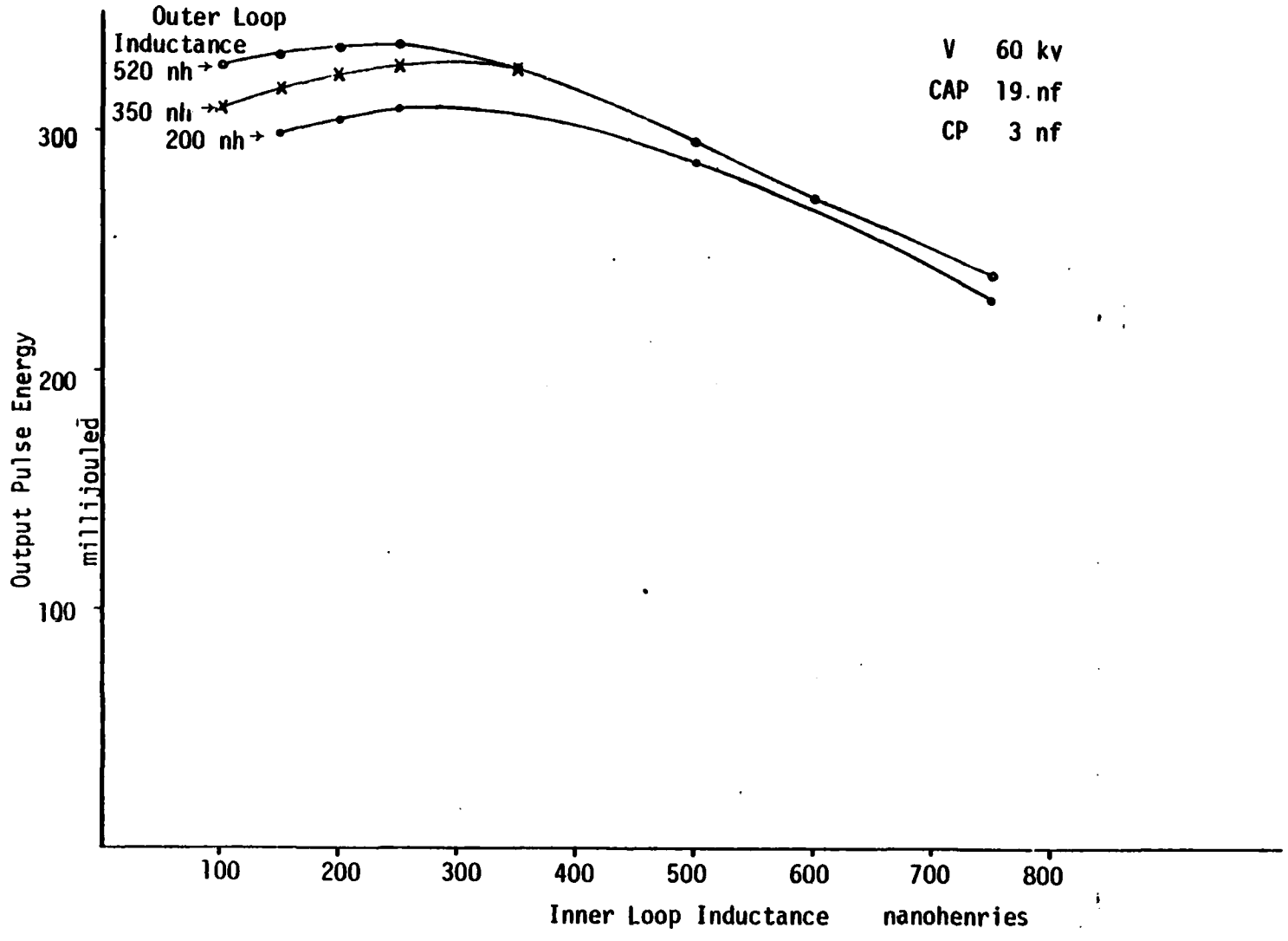

FIGURE 22. VARIATION OF PULSE ENERGY WITH INNER LOOP INDUCTANCE.
Storage Capacitance is Constant.

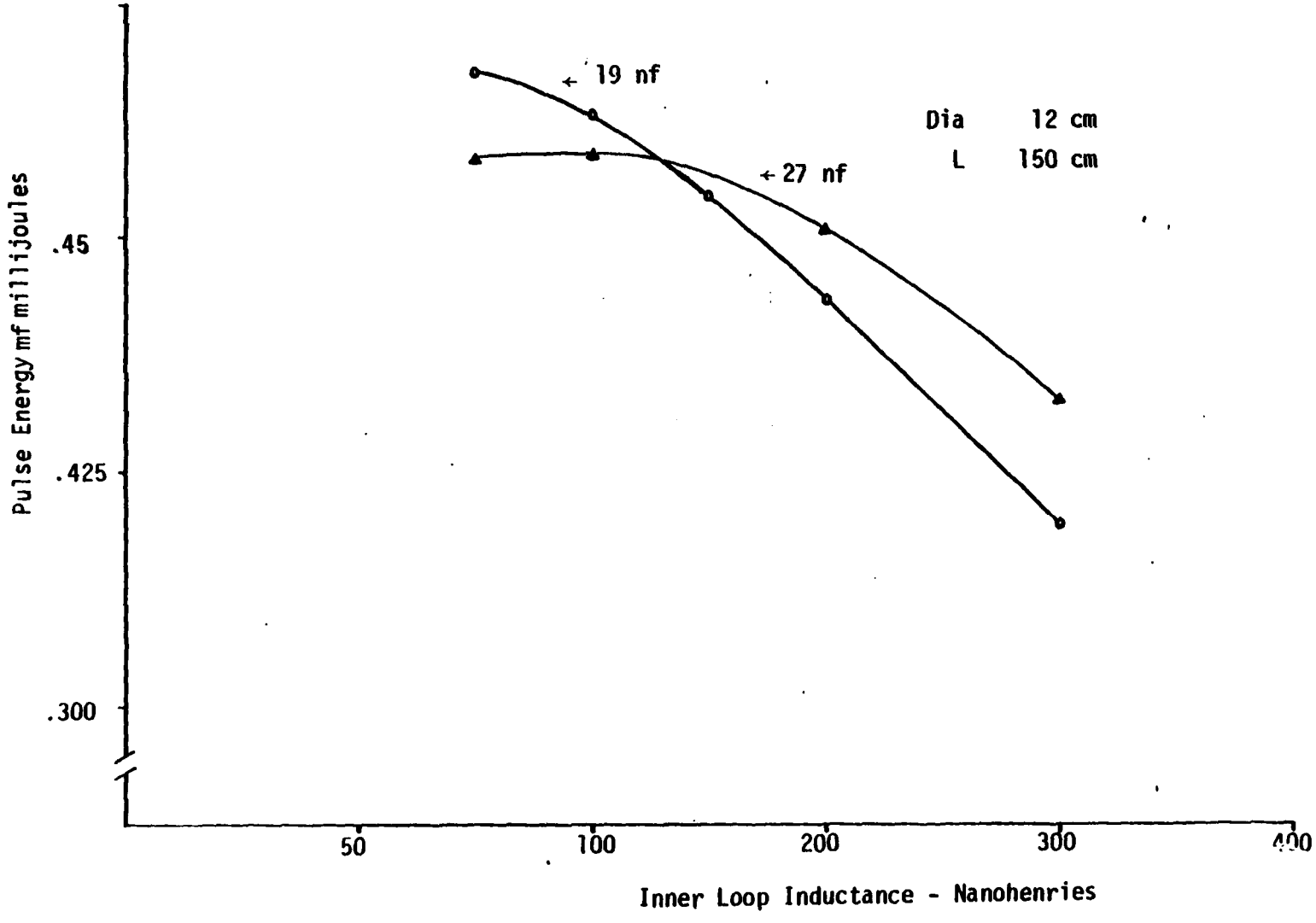

FIGURE 23. DEPENDENCE OF PULSE ENERGY AT 510.5 nm ON ACTIVE LENGTH.
Constant ratio of stored energy to volume (7.6 mJ/cm^3).
Note that efficiency is .9% at 50 cm length and falls on either side.

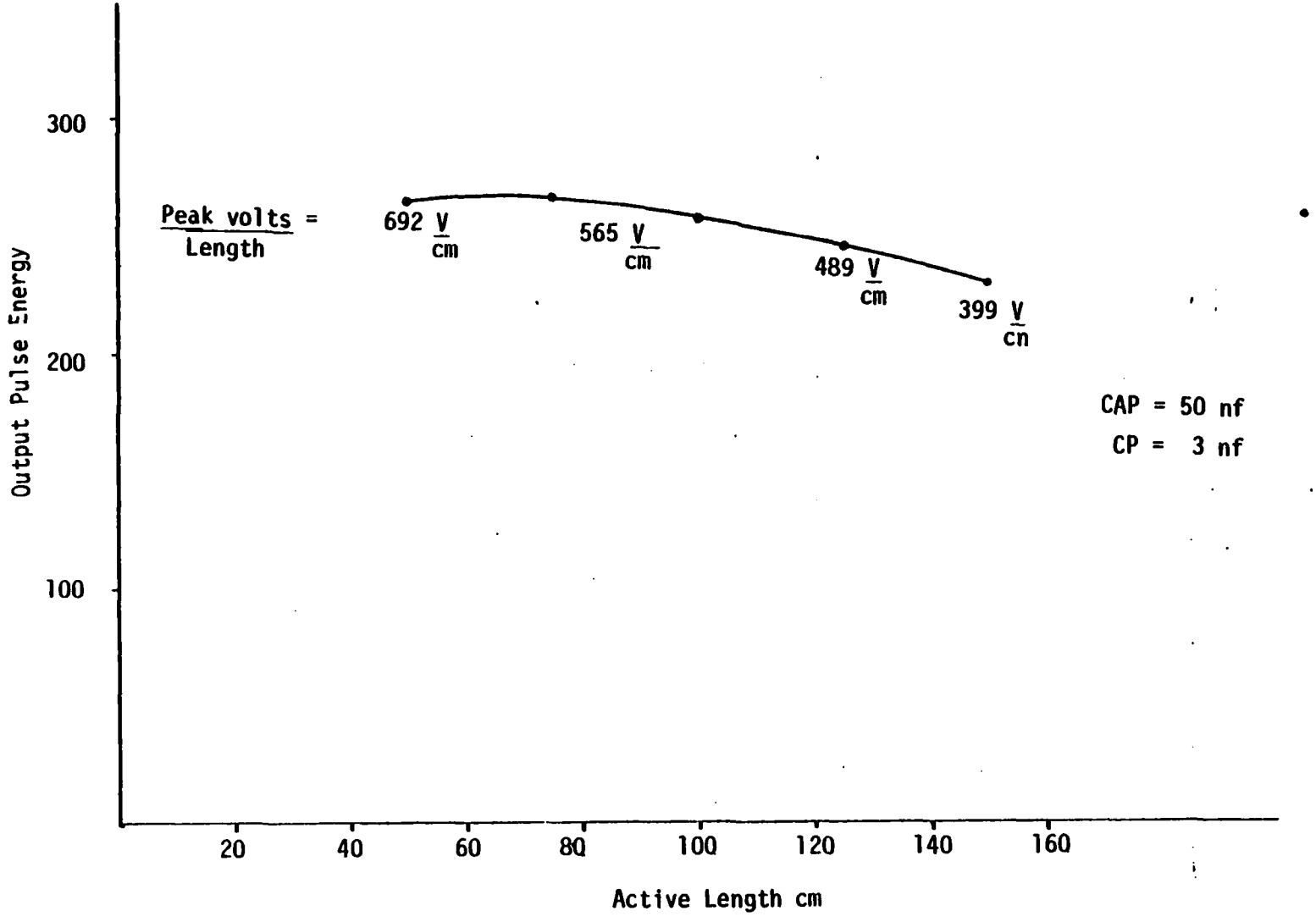

falling as the length increases. Figure 24 shows the output increasing with length and constant field strength, as one would expect.

Reduction of capacitance so as to also keep the specific loading constant would prevent the roll over seen at the longer lengths. Reduction of the storage capacitance to 19 nf at 150 cm active length increases the output to 308 mJ. This is very close to the energy that can be obtained from a projection from short lengths (e.g. a linear projection from 57 cm length gives 297 m J).

Thus, if for experimental convenience one would like to limit the peak voltage to 40 kv, consistent data could be obtained with maximum expectations, if the hot zone were limited to 100 cm.

Finally, variation in output with buffer gas density, copper vapor density, and repetition rate can be seen on Figures 25 through 28.

Figures 25 and 26 show that output increases as the buffer pressure is lowered but tends to level below 10^{17} cm^{-3} (about 25 torr), regardless of electrical parameters applied. Figure 27 shows the output optimizing at a copper vapor density corresponding to about 1430°C. Both are consistent with experimental observations made in smaller diameter tubes.

The repetition rate dependence shown on Figure 28 has little direct data for comparison so it bears some discussion.

Optimum output can be seen to be at a kilohertz for 20 kV applied, about 100 HZ for 40 kV and 20 HZ for 60 kV. The ionization left over at the end of the interpulse period at the optimum repetition rate for each of these voltages is given on Table 8. This ionization is consistent with the model that there is a certain ionization (p) that must be obtained in a fixed period of time for optimum output. Such ionization growth is given by

$$p = b \exp (a V)$$

where b is the ionization at the end of the interpulse period and the beginning of the next discharge pulse

FIGURE 24. DEPENDENCE OF PULSE ENERGY ON ACTIVE LENGTH.
Constant ratio of storage capacitor voltage to active length (400 V/cm).

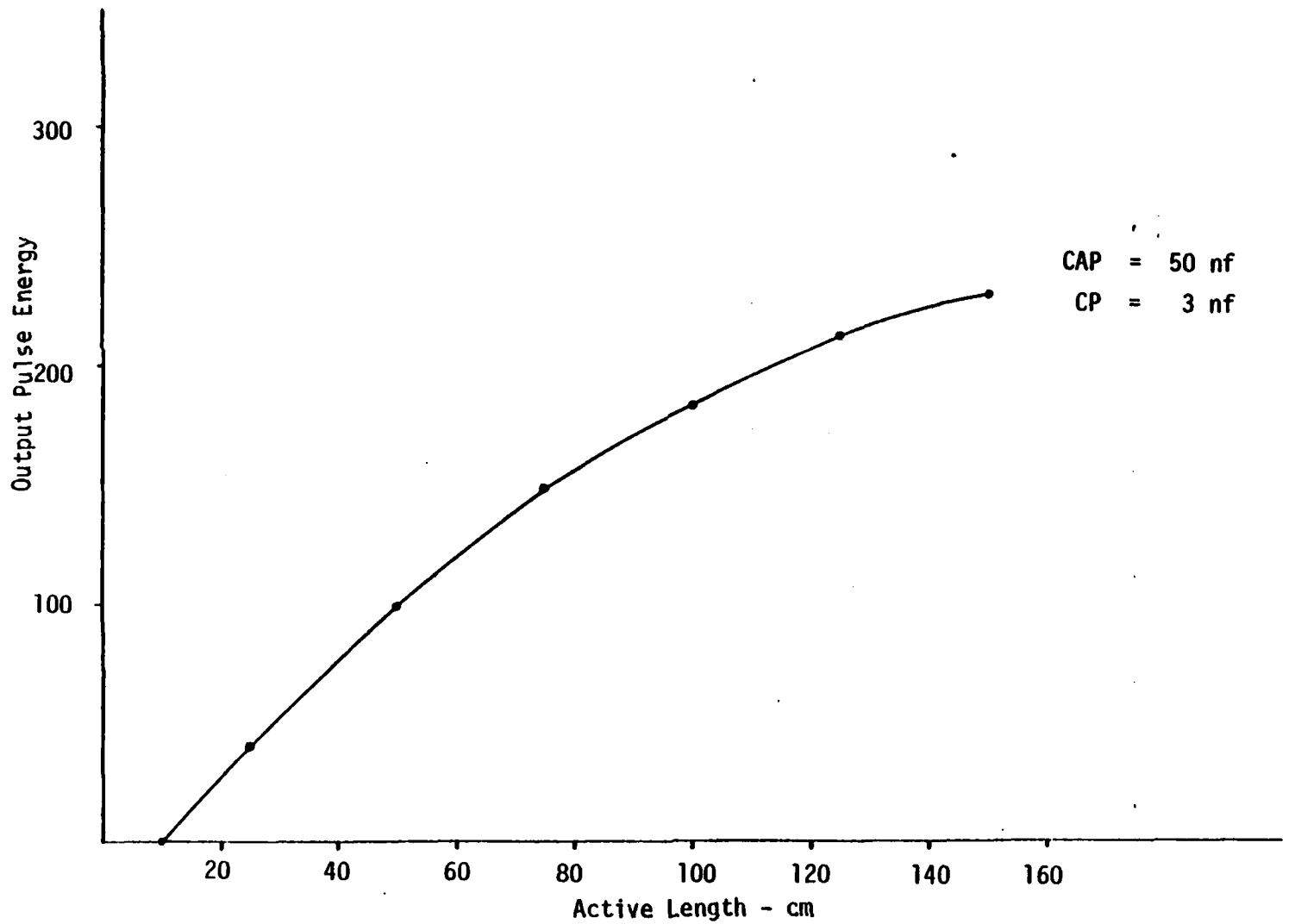

FIGURE 25. PULSE ENERGY OUTPUT AT 510.5 nm AS FUNCTION OF NEON DENSITY

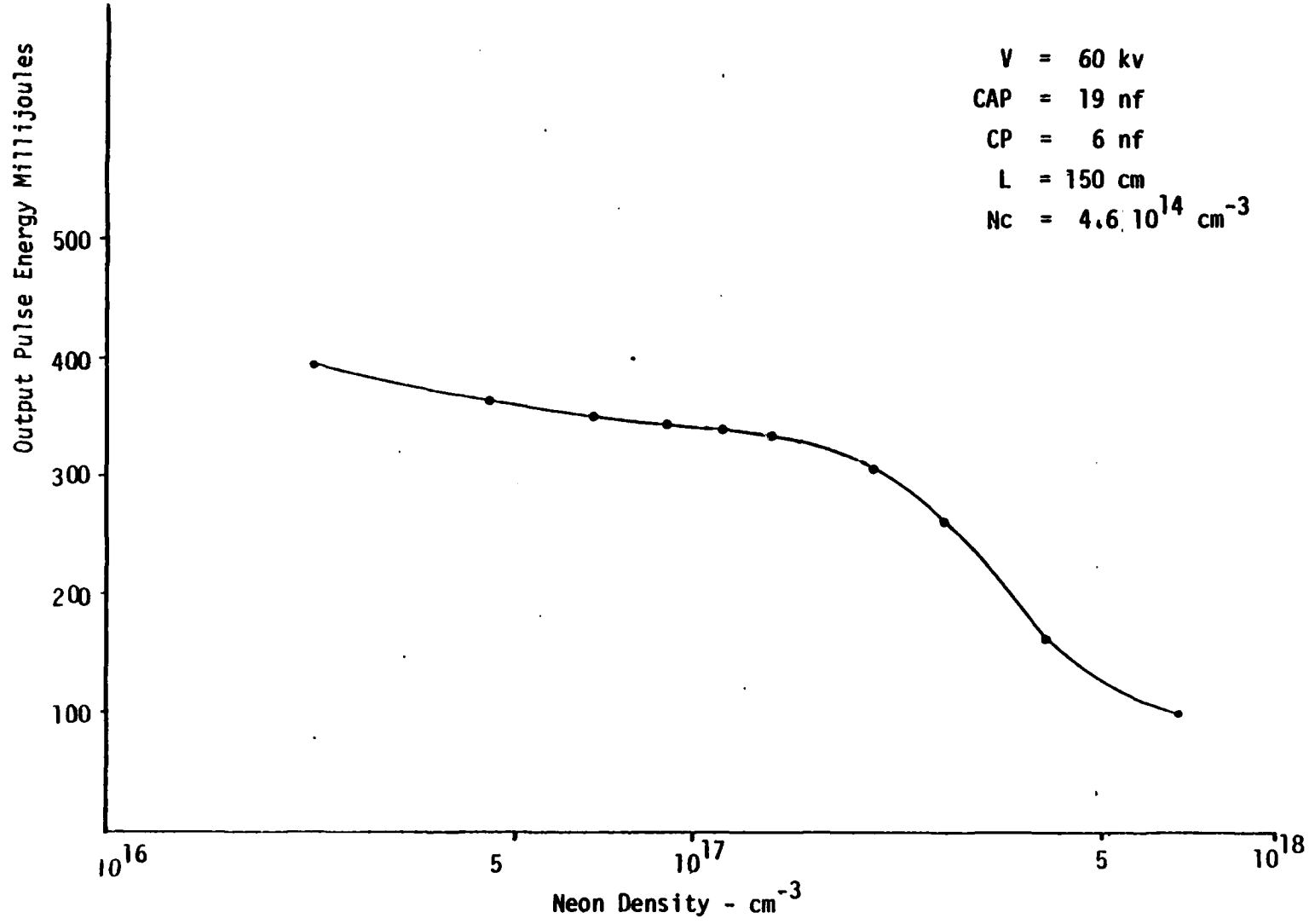

FIGURE 26. PULSE ENERGY OUTPUT AT 510.5 nm AS FUNCTION OF NEON DENSITY

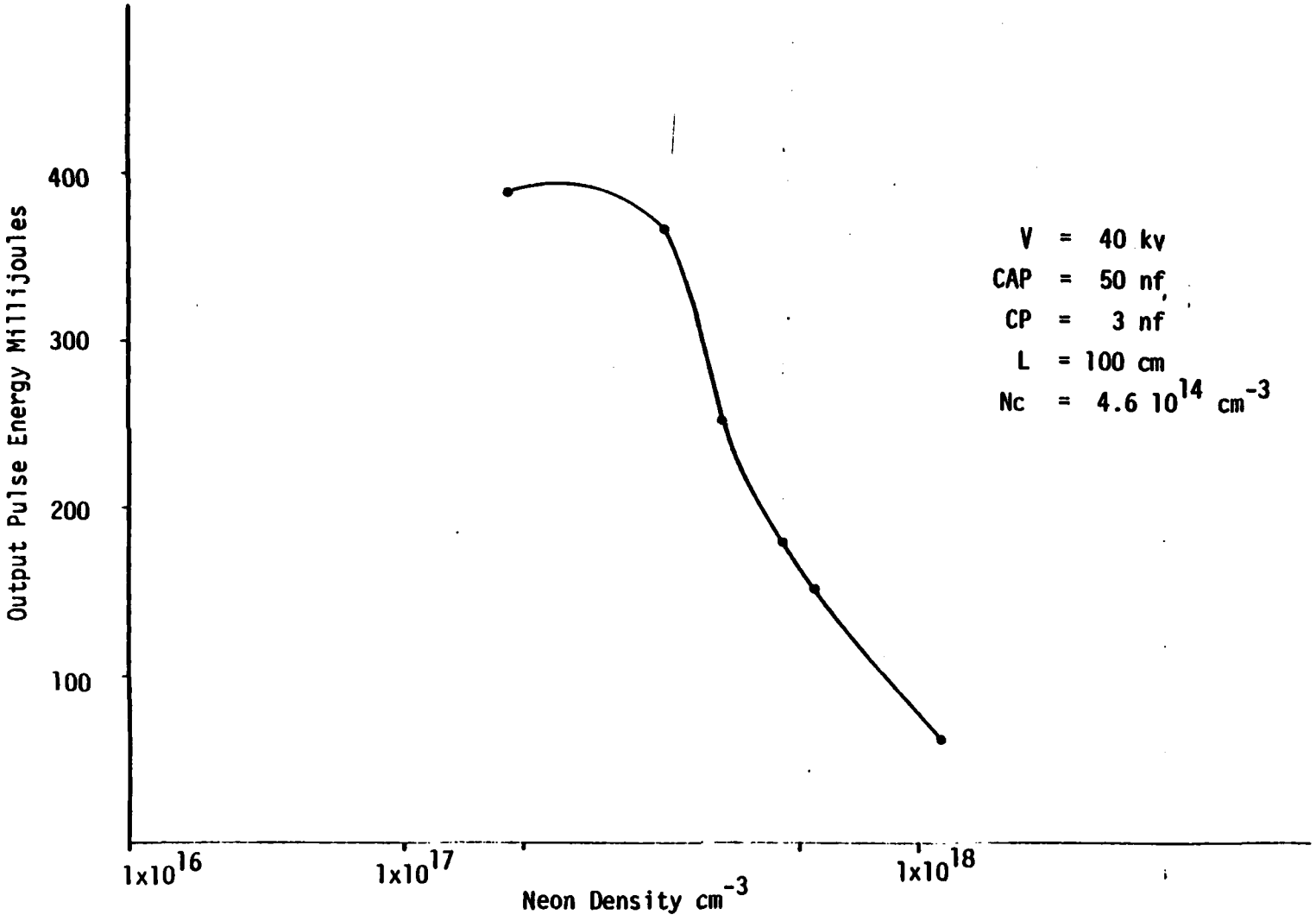

FIGURE 27. VARIATION OF OUTPUT AT 510.5 nm WITH COPPER VAPOR DENSITY

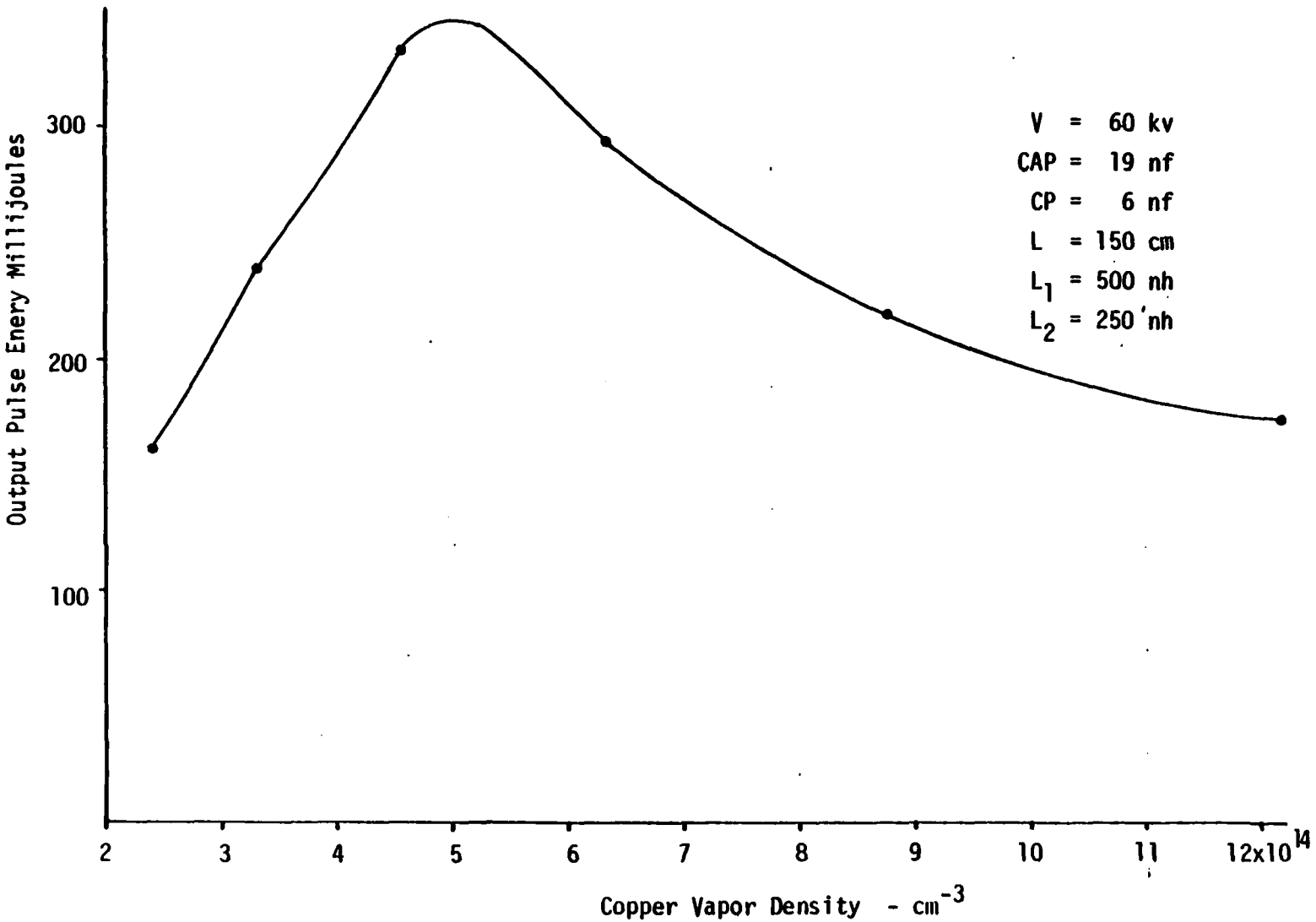

FIGURE 28. VARIATION OF OUTPUT AT 510.5 nm WITH REPETITION RATE AND STORAGE CAPACITOR VOLTAGE

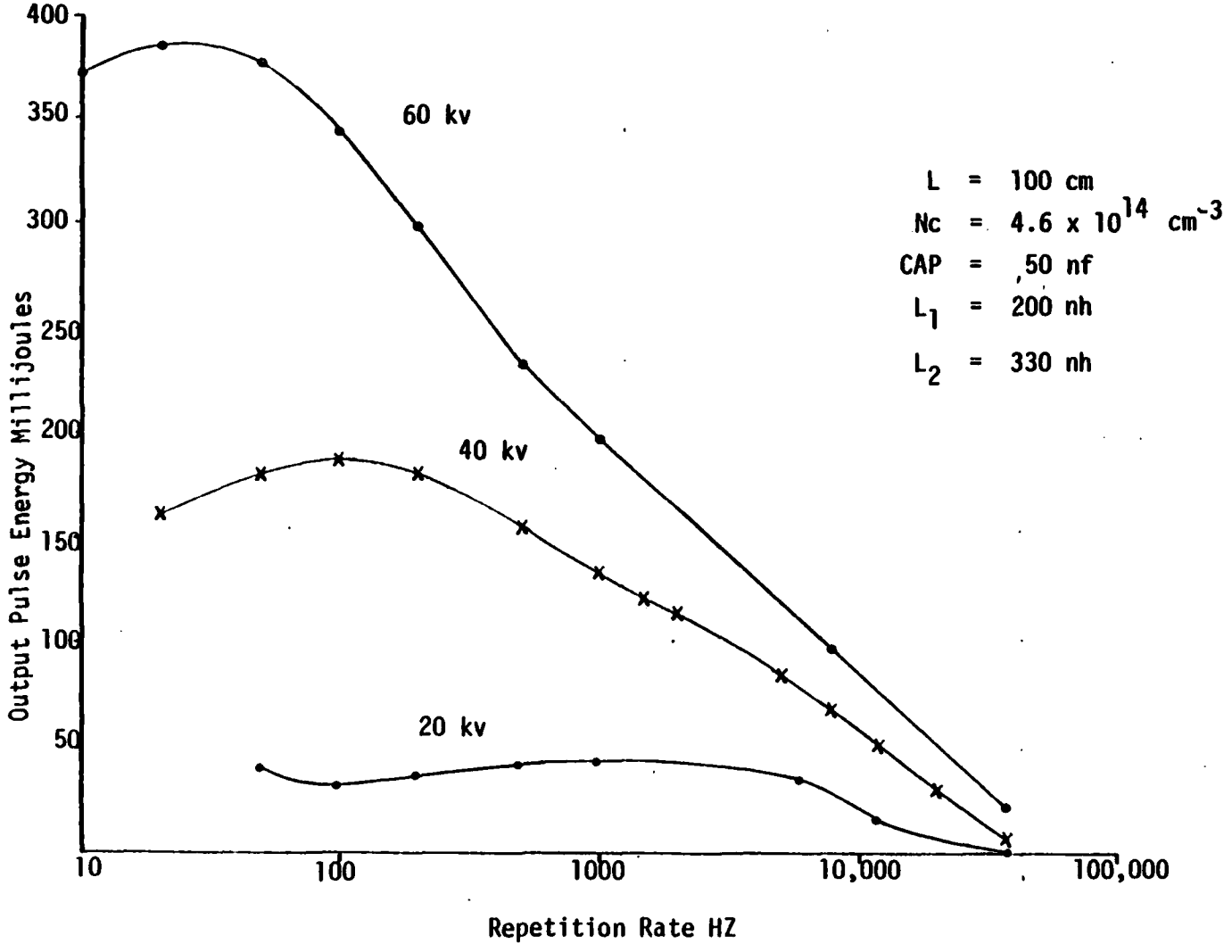

TABLE 8

ELECTRON DENSITY AT OPTIMUM RATE

Voltage (V)	Electron Density at end of interpulse period for optimum rates	Optimum Repetition Rate
60 kV	$4.7\ 10^{11}\ cm^{-3}$	20 HZ
40 kV	$1.93\ 10^{12}$	100
20 kV	$7.97\ 10^{12}$	1000

a is essentially the voltage independent ionization rate and therefore a function of time, length, etc.

V is the voltage

The value of a determined by using all three pairs from Table 8 is essentially identical (.0706, .0709, .0708) leading to an "optimum" ionization of

$$p = 3.3 \ 10^{13} \ cm^{-3}$$

This is the value of peak ionization simulated here, simulated at LLNL and measured at LLNL for high rate optimized large bore lasers.[9,13] Much higher values lead to suppression of the electron temperature and lower values to insufficient upper state pumping.

Evidently very high voltages can be used if the interpulse ionization level has been allowed to fall sufficiently. Then the high voltage can heat the electrons to higher temperatures before the ionization builds up to optimum levels, producing a better inversion and more output.

This argument is developed further in reference 15 for lasers with I.D. of 15 cm and peak voltage up to 100 kv. The relationship of the optimum ionization to the plasma resistance is in particular explored there. It is shown that as the plasma resistance falls at higher repetition rates the fraction of the applied voltage that appears across the laser also falls, reducing output.

In addition it is pointed out there[15] that the bulk of power deposition and lasing takes place while the ionization is still relatively low, reducing the effect of skin depth. The conductivity of 4.4 mho/m and a discharge time of 70 n sec, appropriate to this dischange stage lead to a skin depth of 12.7 cm, well above the 5 cm radius studied here or the 7.5 cm radius studied there. Late in those very large bore simualtions, well after the voltage across the laser and laser output power have faller, the conductivity rises to 67 mho/m. The associated skin depth falls to about 3 cm and the plasma phenomena found by Kushner and Warner at high repetition rates could be encountered.[9] The effect is incidental to lasing here, however, and can be ignored.

Skin effect limitations are thus also ameliorated by operation at low repetition rates and high voltages.

B. SUMMARY

The results of this simulation strongly support the empirical projections cited earlier. Output increases with input and field strength (V/l). It weakly increases inversely with inductance. Other parameters have optimum values. The best set of values thus far identified is given below in Table 9.

Similar optimization for efficiency drives the value of capacitance down. Other parameters are about what they are for pulse energy optimization.

TABLE 9

OPTIMIZED 10 cm LASER PARAMETERS

	Optimum Energy - .337J 1.8 %	Optimum Efficiency 2.5% .224 J
CAP	10 nf	5 nf
CP	3 nf	3 nf
L_1	350 nh	500 nh
L_2	200 nh	250 nh
Voltage	60 kV	
Copper Density	$4.6\ 10^{14}\ cm^{-3}$	
Neon Density	$1.4\ 10^{17}\ cm^{-3}$	
Repetition	200 HZ	

V. EXPERIMENT DESIGN

A. DESIGN PHILOSOPHY

The basic design for an experimental facility was guided by the principal of flexibility. Previous experimental programs were hindered by the long time required to get data at a specific temperature with a specific capacitance, voltage, inductance, etc. The long times required to reach a stable thermal condition were, of course, responsible.

Consequently, it was decided to run the laser discharge in bursts of limited duration (up to 100 pulses). The heating would be supplied by an auxilliary technique which could maintain the temperature at a fixed value as the pulsed discharge parameters were changed. This technique had been previously used successfully with auxilliary resistance heating.[4,16,17]

Unfortunately there are several characteristics of resistance heating that cast doubt on its proper simulation of a discharge heated device. First, the temperature distribution is likely to be different. Secondly, the electric field distribution will be affected. Finally, experience shows that a laser heated in this way is susceptible to an increased number of failure modes, a question of major concern when large diameter high cost ceramic discharge tubes are being used.

An alternative heating technique that has none of these shortcomings is the glow discharge. It uses the same gas and electrodes as the pulsed discharge. Only the voltage and duration of the discharge differ. It had been previously tested successfully and its application here was natural.

Other design characteristics such as

1) Insulating outer shell
2) Fibrous material filling the annular region between the discharge tube and shell for both thermal and electrical insulation
3) Free unrestrained ceramic discharge tube to minimize breakage
4) Contaminant free materials
5) Sealed off operation

which are desired in a practical device[1,18] were retained where possible.

To test these design characteristics and associated operational procedures a subscale model of the laser was built first. As a result several modifications were made to the design. Successful glow discharge heating, burst mode discharge operation and lasing were ultimately obtained. Figure 29 shows a photograph of the subscale laser. Table 10 lists its design parameters and Figure 30 a laser pulse obtained with it.

Table 10 also lists some of the design parameters of the full scale laser that resulted. Figure 31 is a drawing of its overall design* and Figure 32 and 33 are respectively photographs of the full laser and of the end containing the capacitor bank and switch.

B. OUTER SHELL

For convenience and strength heavy wall Corning glass process pipe was used as the outer shell of both lasers. O-rings and standard glass pipe flanges were used to mate the glass to the electrode flanges and the window assemblies.

The glass failed once when it was raised locally to over 400°F during the passage of an arc near the wall as part of an insulation failure. During proper operation the glass surface reached a uniform 200°F only when the inner tube was heated to over 1400°C and so was well within safe limits.

The dimensions of the glass were by no means uniform. However, an adequate fit was generally obtained between the OD of the machined insulation and the glass to prevent propagation of a discharge. This was true for all versions of the subscale laser and the first glass pipe used for the full scale laser. However, the second 9" glass pipe evidently did not provide an adequate fit for the insulation. During pulsed discharges some streamer channels could be seen. The d.c. glow was never visible, however, because much lower voltages were used.

---

* This drawing was supported by GE IR&D so that amplifier modules could be easily made at a later time.

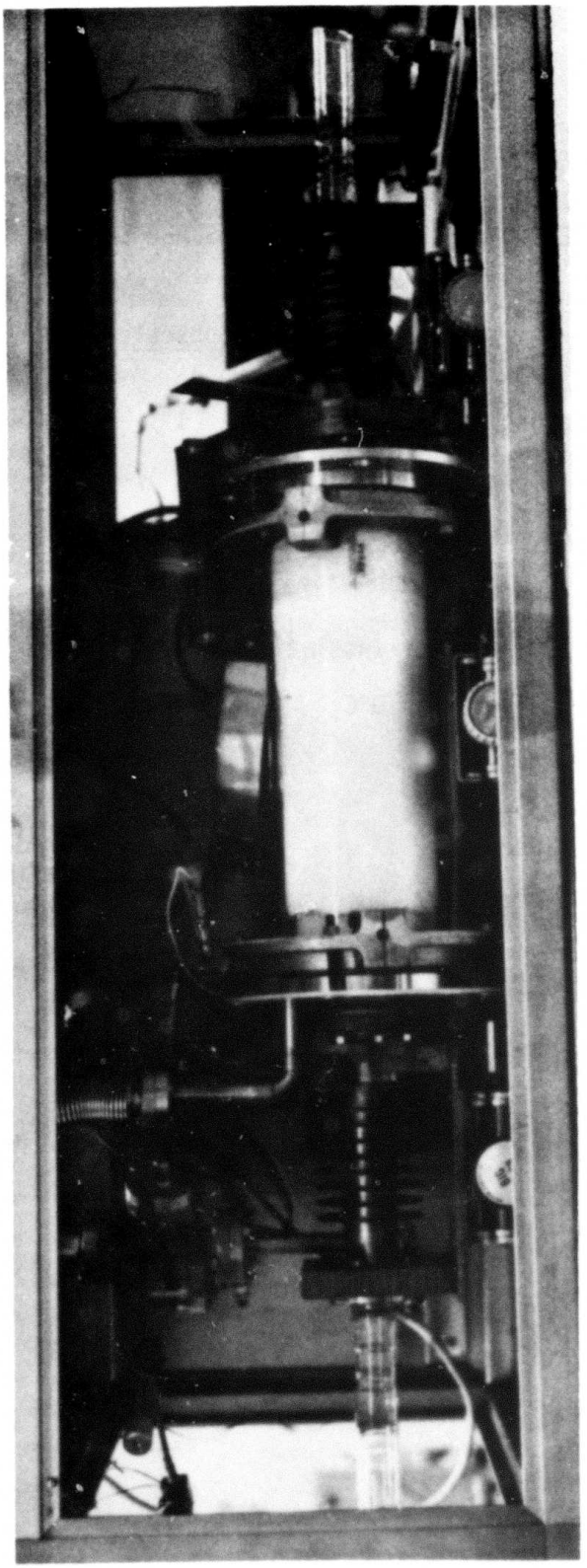

FIGURE 29. SUBSCALE MODEL OF SCALE DEMONSTRATION LASER TECHNOLOGY

TABLE 10

DESIGN PARAMETERS OF SUBSCALE AND FULL SCALE LASER MODELS

	Subscale	Full Scale
Discharge Tube ID	1"	4 1/8"
Outer Tube OD	2 1/4"	5 1/4" *
Hot Zone Length	30 cm	101 cm
Total Length	58"	107"
Outer Diameter of Insulation	6"	9"
Power to reach 1470°C	880 W	6500 W
Resonator		
Transmitter	2" clear flat	6" clear flat
Reflector	2" dia. 10m rad. Dieletric coating	6" dia. 20m rad Silvered coating

* Not used except during Preliminary Tests

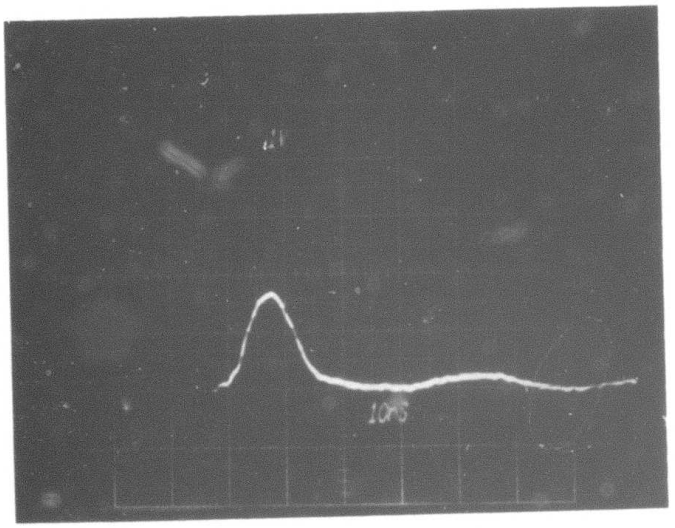

FIGURE 30. LASER BURST OBTAINED WITH SUBSCALE LASER MODEL

FIGURE 31(a) DRAWING OF EXPERIMENTAL 4" COPPER VAPOR LASER (RIGHT HALF)

FIGURE 31(b) DRAWING OF EXPERIMENTAL 4" COPPER VAPOR LASER (LEFT HALF)

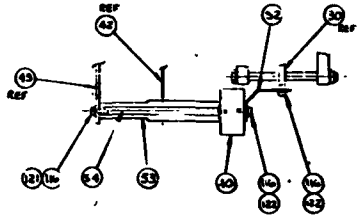

VIEW C-C
TYP 14 PLCS

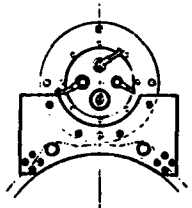

VIEW A-A

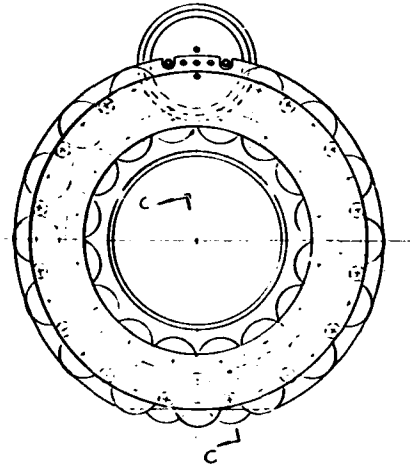

VIEW B-B

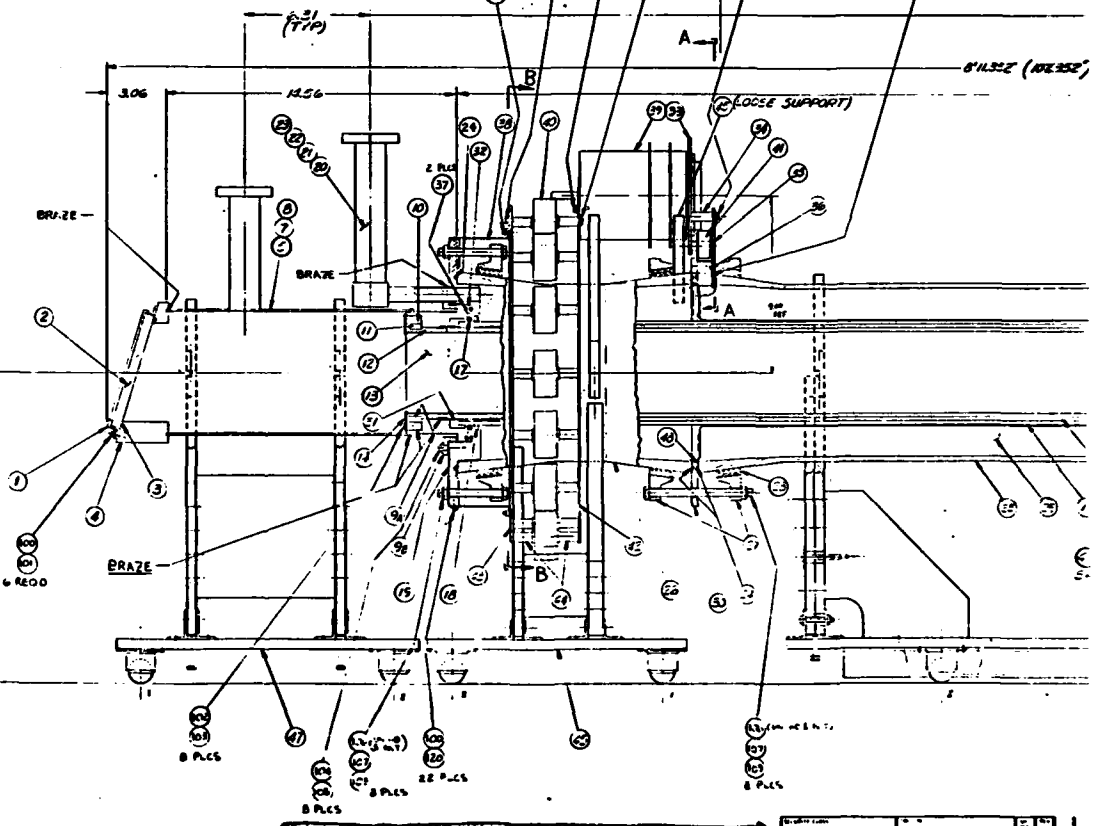

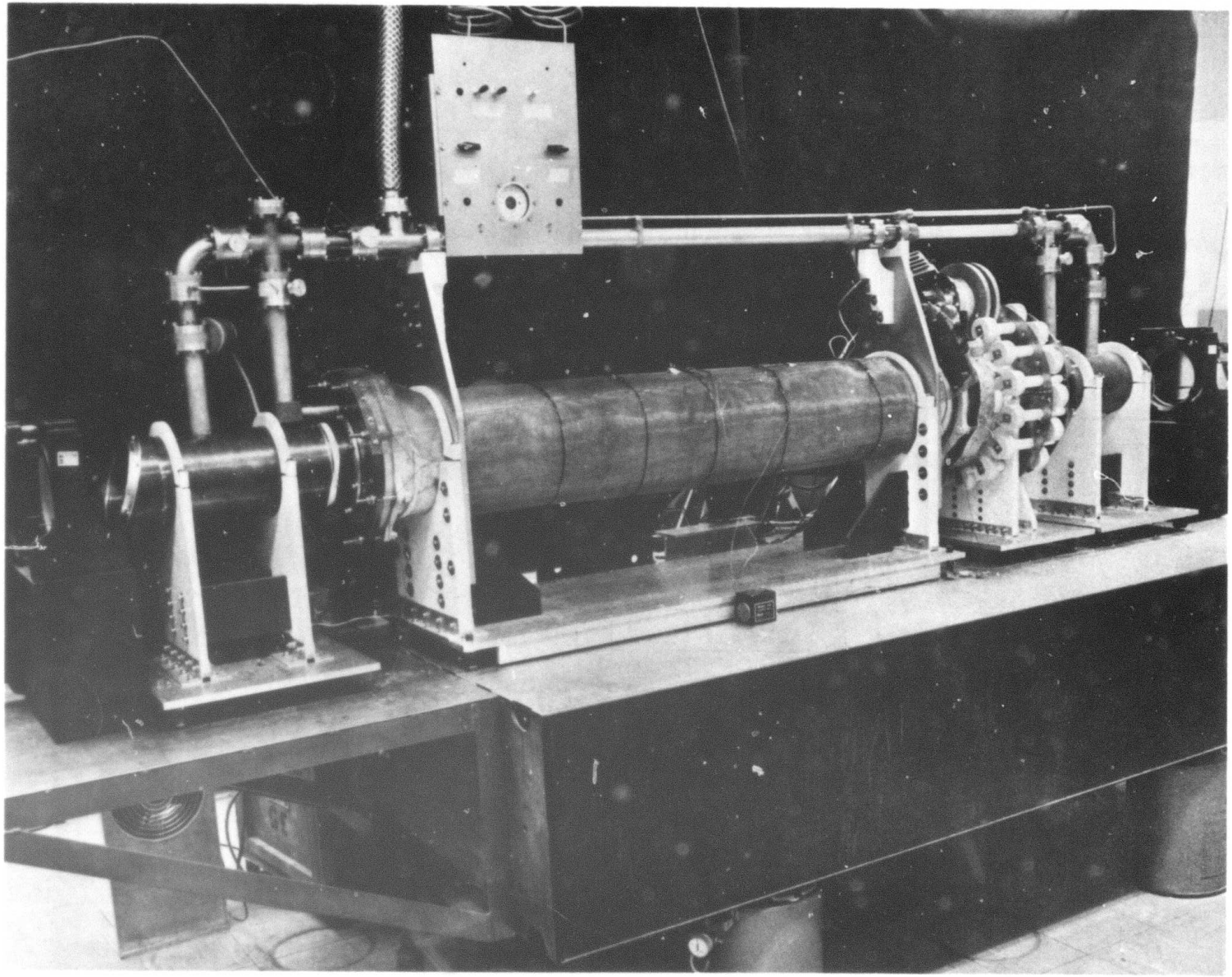

FIGURE 32. PHOTOGRAPH OF LARGE DIAMETER COPPER VAPOR LASER SCALE DEMONSTRATION FACILITY

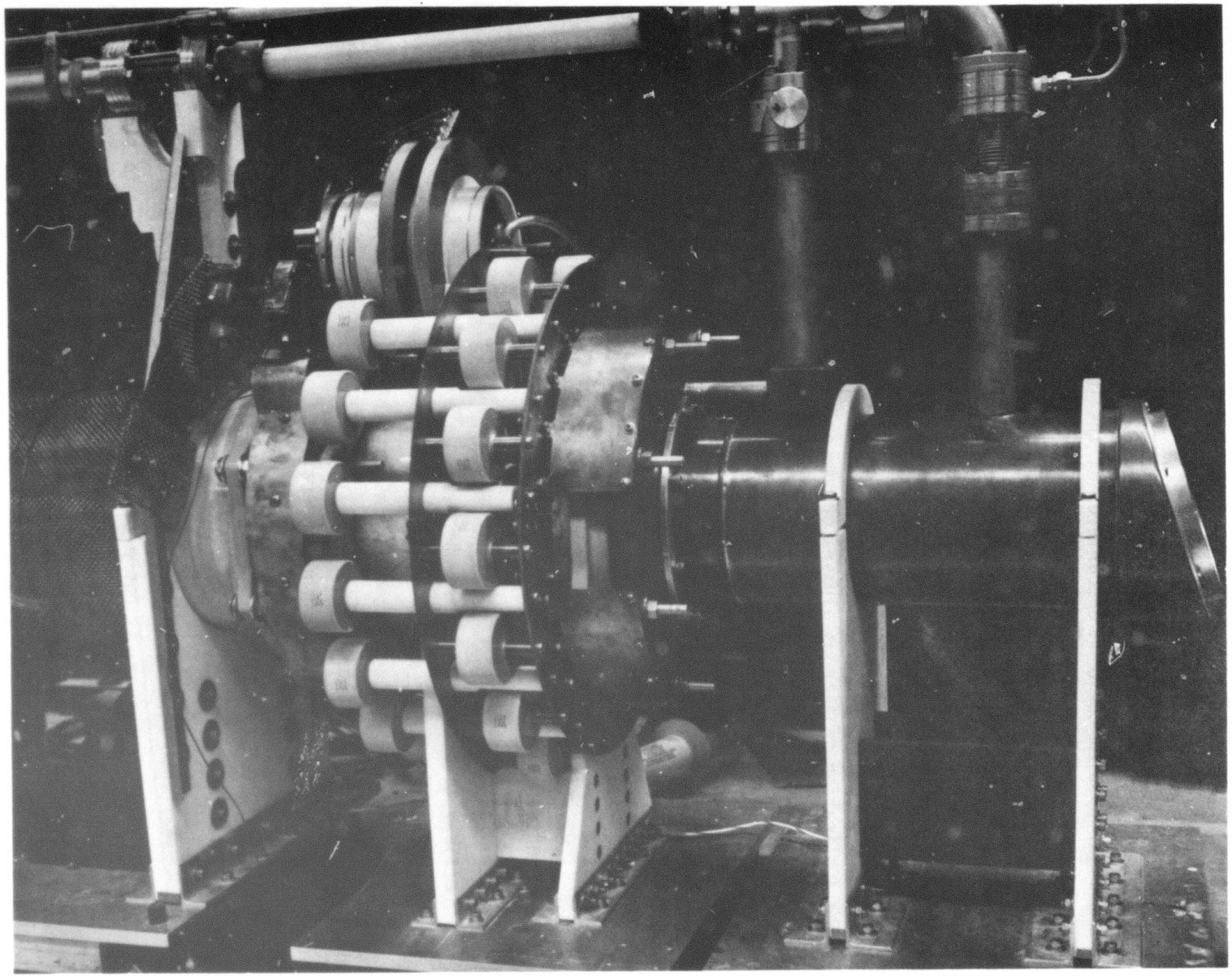

FIGURE 33. PHOTOGRAPH OF SCALE DEMONSTRATION FACILITY CAPACITOR BANK AND SWITCH

A similar problem could be encountered at the interface between the ceramic tubes and fibrous insulation. The large 4 1/8" ID and 5 1/4" OD alumina tubes were quite out of round. However, a blanket of saffil fibers was wrapped around the outer tube and the whole assembly was forced into the fibrous zirconia insulation. In this way the saffil expanded to fill the non uniform gaps.

C. FIBROUS INSULATION

The application of fibrous alumina or zirconia [19] as insulation was first used at GE sometime ago. This concept evolved into a design in which the discharge tube is freely supported inside of nested tubes of tubular insulation which in turn fit snugly into an insulating outer envelope[1,18]. In this position the fibrous material acts as a thermal insulator to control the temperature of the discharge tube and as an electrical insulator to insure that no discharge current passes through the annular region outside of the discharge tube.

As just described, glass pipe was used for the outer envelope in these experiments.

Zirconia was found to be the fibrous material of choice because of its outgassing properties, to be discussed elsewhere, as well as its better known insulating properties. The inner saffil layer described earlier provided the thermal drop necessary to insure that the alumina (saffil) zirconia interface is well below 1400°C. Experiments have shown that an exothermal reaction can be initiated between the two materials if the temperature is above 1400°C.[20]

D. SEALED OFF OPERATION

Ideally the laser should be sealed off with no buffer gas flow. In a copper vapor laser such flow is not necessary for thermal rejection or replenishment of the medium. However, it has often been used in this country to simplify laser construction. Still, the earliest nested insulator tests were sealed off.[18]

The large bore facility constructed here could not be truly sealed off because of the necessity for easy modification. However, it was made carefully and leak checked so as to minimize introduction of atmospheric gases during short term sealing. Rate of rise tests gave approximately 1μ/hr. rise. This would introduce impurity levels of less than 30 ppm in one hour, far below levels previously found to interfere with laser operation.

Sealing of one section of the laser from another was also considered in order to avoid the difficulties associated with bake out of the fibrous insulation described in the following section. Thus some subscale model tests and initial operation of the full scale laser were accomplished with a nested ceramic tube design. The inner tube acted as the discharge tube and rested freely on saffil within the outer alumina tube. The outer tube had O-rings on the ends of its outer surface isolating the gas within the two ceramic tubes from the fibrous insulation. This concept is shown on Figure 31.

In this design the insulation could be evacuated while buffer gas was present within the discharge tube.

No contamination could move between these isolated regions, eliminating bakeout requirements for the insulation.

This could not be a long term solution, of course, because of the presence of O-rings and their eventual contamination of any sealed off system. However, as a time saving expedient for these tests it appeared to be useful.

The technique proved effective for the subscale laser. The small (2") outer tube was sufficiently round so that the O-ring sealed well and thermal stresses never led to breakage. Levels of contamination that otherwise took a week of baking were reached overnight.

Unfortunately the application of this concept to the full scale device was unsuccessful. The large (4 1/8" and 5 1/4") ceramic tubes were considerably out of round and there was evidence that they were mechanically weaker than the small tubes. It took one of the manufacturers (Coors) several tries to get a

tube that did not fail during firing. Worst off all two outer tubes failed in the final stages of heat up after only a few heating cycles. The cause appeared to be related to inability of the tubes to handle the stresses imposed upon them by the seals at each end.

As a result of this breakage the full scale laser design used during testing involved only the single ceramic (discharge) tube freely supported in fibrous insulation. Its ends were unrestrained and contamination evolved by the insulation could enter the discharge tube. Consequently, the special efforts developed previously for bakeout of the insulation were employed.

E. CONTAMINATION

A major effort was directed toward reduction of contaminant levels within the laser. This was principally motivated by the observation that contaminant levels commonly present in copper vapor lasers could be associated with limitations in the voltage that could be applied. The limits could be identified by a persistent latching of the thyratron switch with the application of voltage levels, or the introduction of contaminant levels beyond some value. Analysis of current and voltage waveforms pointed strongly to constriction of the discharge immediately preceding the latching.

Such a correlation of molecular contaminants with increased tendency toward constriction has been previously mentioned in the literature.[21,22,23] While ionization and cathode sheath instabilities are commonly mentioned as the cause a unified model is not yet available. Consequently the work here was empirical in nature.

The need to extend the usable range of voltages can be seen by comparing the requirements given in Section IV (40-60 kv) with the maximum values of about 20-25 kV typically used.[4,6,9]

Examination of early successes with high voltages in this laboratory showed that special concern with the outgassing properties of the materials used was common to them. Consequently a series of studies were undertaken with the

TABLE 11

RESPONSE OF VARIOUS MATERIALS OF CONSTRUCTION TO BAKING

Material	Mechanism for Liberation of Contaminants	Response to Baking*
Insulation		
Fibrous Alumina (ALC)[19]	Heating	-
Fibrous Alumina (AL30)[19]	Heating	0
Fibruous Zirconia (ZYC)[19]	Heating	0
Electrodes		
Molybdenum	Discharge Attachment	+
Tantalum	" "	+
Window Assemblies		
Stainless Steel	Discharge Attachment	-
Copper	" "	-
OFHC Copper	" "	+
Discharge Tubes		
99.8% Alumina (McDanel)	Heating	0
99.8% Alumina (Coors)	Heating	0

*
- \- Could not outgas with baking
- 0 Could outgas with extended bakeout
- \+ Could outgas with short bakeout

subscale laser in which spectral intensities of contaminant lines were monitored as various materials of construction were used and outgassed for various periods of time. A similar study has been done previously[18] and provided a basis for this work. Table 11 lists materials tested, the mechanism which liberated contaminants, and their response to baking.

Of the components listed in the table the fibrous insulation required the most effort to thoroughly decontaminate. Its porous nature provided a large area for absorption. In addition there was evidence that some component in the manufacture evolved gas as it was heated. The ALC insulation could not be sufficiently outgassed for sealed off operation. The AL30 and to a lesser degree the ZYC required many hours. The ZYC zirconia was chosen for use in the full scale laser.

Outgassing of window assembly materials was only a consideration when discharge currents extended into that component. Experiments here and in the GE Lamp Glass Department have shown that there are dissolved gasses, even in stainless steel, that are released by such discharge attachment. Baking does not affect such dissolved gasses. While pressures of 30 torr or above tended to confine discharge currents within the electrodes, it was considered wise to make window assemblies out of a metal that would minimize outgassing. OFHC copper was chosen for use in the full scale laser.

Several different baking techniques were used. They included pulsed discharge heating with flowing buffer gas glow discharge heating with flowing buffer gas, and resistance heating with an element placed inside of the evacuated discharge tube. All three were effective but each had different shortcomings. The pulsed discharge required operator attention, particularly after the power had just been raised, because of the constant threat of thyratron latching. The glow discharge was clearly superior but also had the possibility of arc transition with attendant electrode damage. The resistance heater used tungsten wire and

was susceptible to oxidation; furthermore, it had to be removed before discharge operation could begin, thus exposing the laser to air and requiring further baking.

As a figure of merit the strongest contaminant line, hydrogen atom 486.1 nm, was monitored as before[18]. When the laser was heavily contaminated (using an arbitrary scale, intensity $\gtrsim$ 100) no attempt was made to operate the laser at high temperature since even discharge color betrayed its contamination. As a typically clean condition (intensity ~ 10) was approached discharges could be run with increasingly higher voltages without constriction. Typically this meant 10-20 kV could be applied to the storage capacitor. Finally, exceptionally clean conditions (intensity $\lesssim$ 1) allowed voltages as high as 49 kV to be discharged without thyratron latching. This last result was obtained over a 30 cm electrode separation in the subscale laser, indicating that a similarly constructed large bore device could be operated in the same way.

F. GLOW DISCHARGE HEATING

A glow discharge heating technique had been demonstrated before the beginning of this program.[24] Allthat it used was a DC or AC power supply with a ballast resistor or inductor in series with the laser load. The discharge then passed through the laser attaching to electrodes in the same way as the pulsed discharge does. In fact the appearance of the discharge is identical.

The 60 HZ AC tests had the advantage that an inductor could be used to provide the ballast, thus causing all power dissipation to be inside the laser. The DC source on the other hand needed a cooled resistor. Unfortunately suitable high current inductors were not available and so DC supplies with resistance ballast had to be used.

The glow discharge heating technique was applied in the subscale laser both for bakeout and as a heater for laser tests. Bakeout operation required caution at high power levels because the electrodes could be damaged by transitions from a glow to an arc. Low power operation presented no such limitation, a

fortunate fact since the discharge at low temperature invariable had a constricted form. Once temperatures of several hundred °C were reached however, the discharge became diffuse and could be maintained there if the molecular contaminants concentration was not too high. This was often controlled by using a fast flow of the helium buffer gas.

Initial cold, high contaminant operation required higher voltages, lower currents and higher buffer resistance than later high temperature operation. Thus, provision had to be made for switching of the buffer resistors involved. Figure 34 shows the switch arrangement.

For initial breakdown and contaminated operation S_1 and S_2 were open and S_3 was closed. This gave DC supply #1 a 9600 Ω series resistance sufficient to prevent current run away as the discharge resistance fell during laser clean up. Since the 9600 Ω bank could not handle current above 3/4 amp without overheating, switch S_1 had to be closed leaving only the 800 Ω bank as a buffer. When more than 3 amps were needed switch S_2 was closed and power supply #2 turned on. In this way up to 6 amps of current could be provided to the large bore laser.

Laser discharge operation required that the heating current be turned off briefly. This allowed metastables created during the DC discharge to die away. Then opening S_3 isolated the laser anode so high pulsed voltages could be applied for laser operation.

After a laser burst or two switch S_3 could be closed and the heating current continued to prevent laser cooling.

G. PULSE DISCHARGE COMPONENTS

The pulsed discharge circuit used was essentially identical to that developed udring previous work in this laboratory.[25] It differed primarily in the components used and the low inductance configuration in which the capacitors and thyratron were arranged. Figure 35 shows the circuit and the values of the different components in the full scale laser. Figure 33 shows how the

Figure 34. D.C. Glow Discharge Circuit

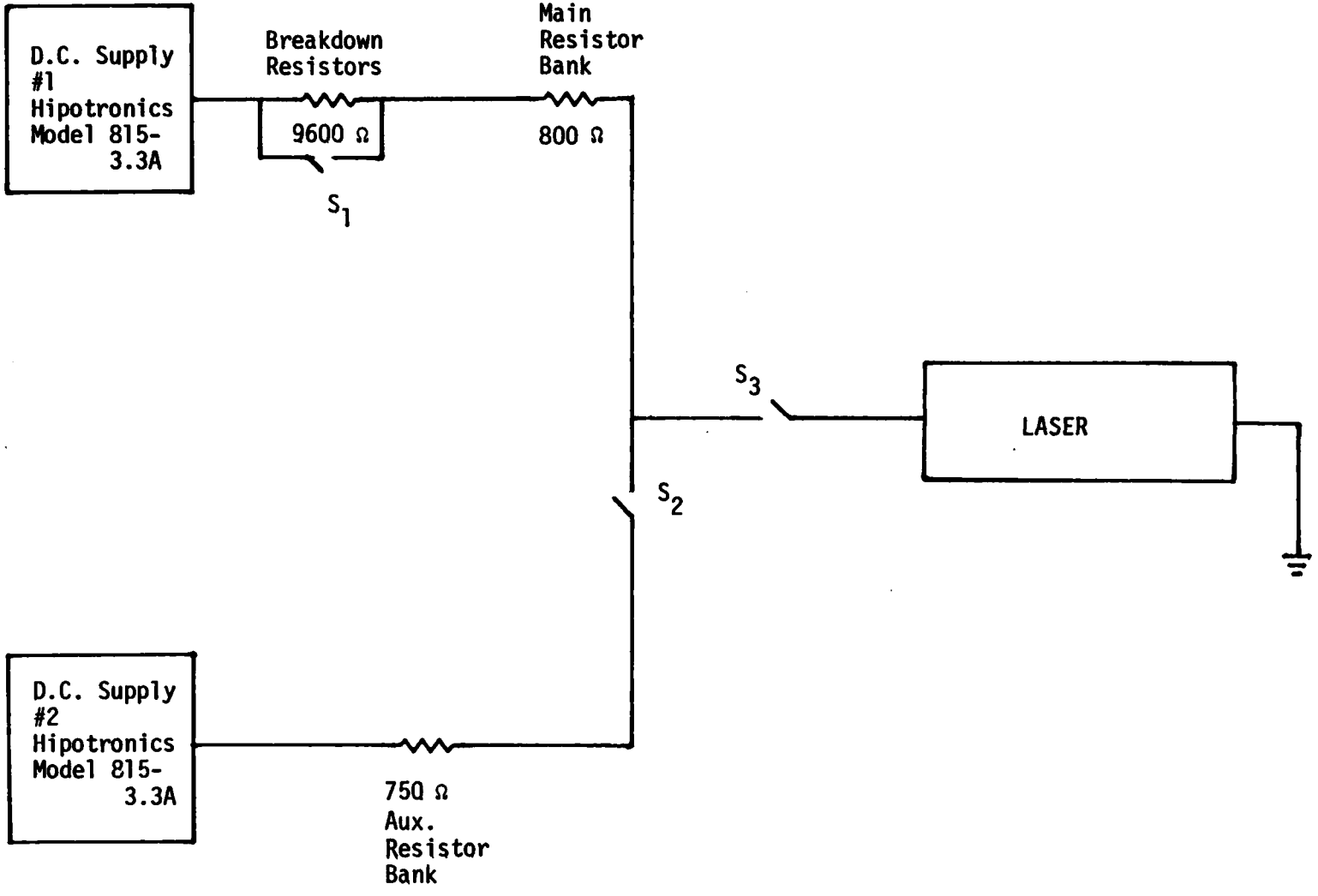

Figure 35. Pulse Discharge Circuit

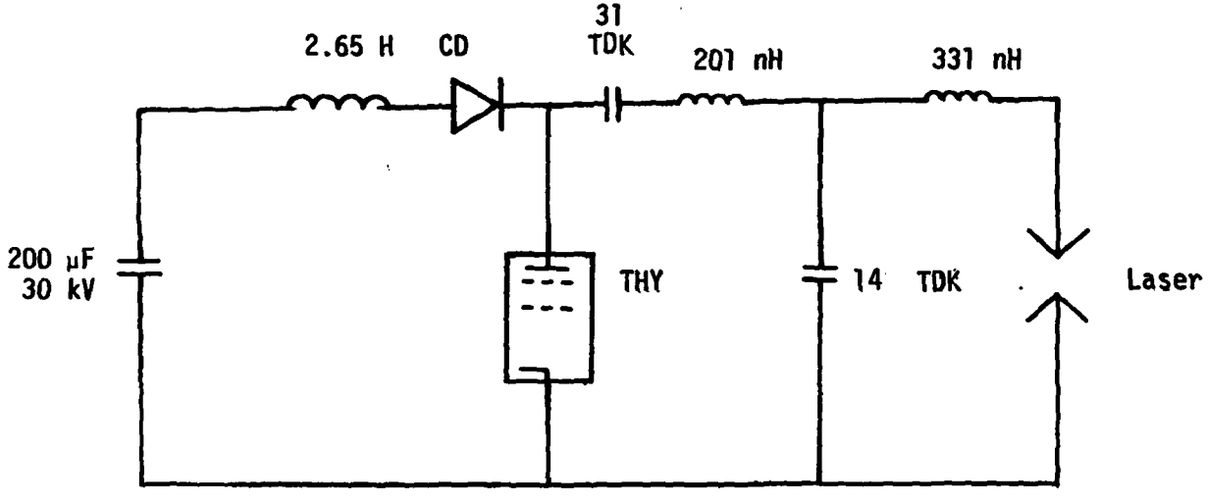

THY	Thyratron Egg HY5312
CD	22 Varo VC80X Diodes
CD	Maximum of 31 TDK Capacitors S940 1.7 nf 50 kV
14 TDK	Maximum of 14 TDK Capacitors S940 1.7 nf 50 kV

FIGURE 36. EXPERIMENTAL LAYOUT SCHEMATIC

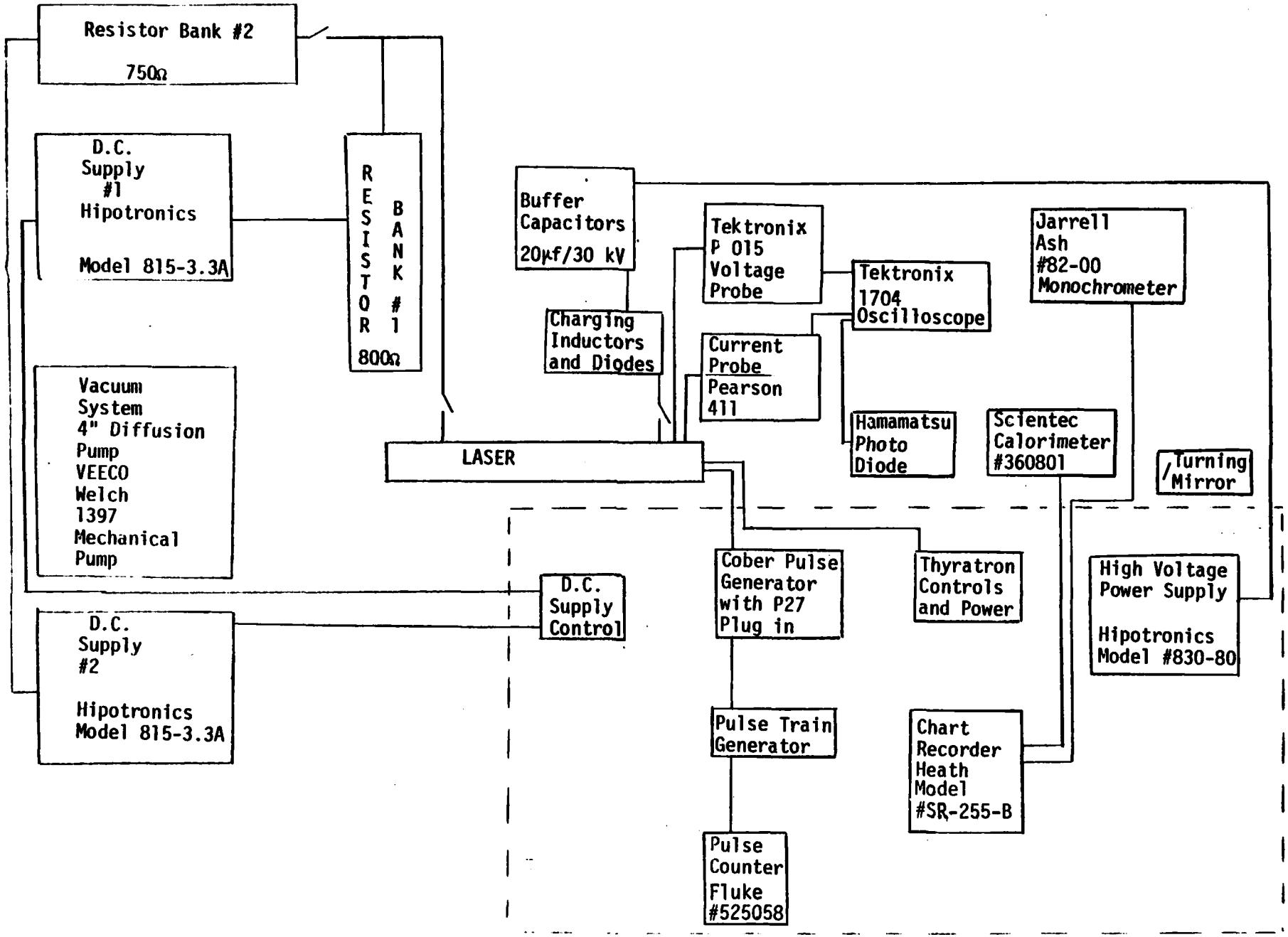

capacitors and switch were arranged so as to give minimum inductance. The inductance values given on Figure 35 were computed from geometrical considerations.

The discharge capacitors were strontium titanate units manufactured by TDK Corp. Their small size for such a high capacitance and highvoltage stand off capability determined the low inductance.

The thyratron was a modified EG&G HY5312. The modification, conducted under a GE IR&D program, was the addition of two collars around the alumina body to extend the high voltage stand off capability of the switch. A similar device had been used in oil at up to 60 kV though the manufacturer cautioned us that voltages above 50 kV might damage some units.[26]

Several tests were conducted at up to 50 kV with these components and successful discharge operation was obtained.

H. EXPERIMENT LAYOUT

The schematic layout of the full scale laser experiment is shown on Figure 36. Included are several pieces of diagnostic equipment that were used during the course of the work. In particular note the Tektronix 1704 oscilloscope which has a bright enough trace that single traces of even 10 ns/cm sweep can be photographed.

VI. RESULTS

A. GLOW DISCHARGE HEATING

The 4" laser was cycled from room temperature to almost 1500°C many times using the glow discharge heating technique. It proved itself to be reliable and consistent even under adverse conditions.

The discharge characteristics were, of course, heavily dependent upon contamination, electrode condition, etc. but relatively consistent data ($\pm$ 6%) could still be obtained once the bulk of the molecular contamination was gone. Figure 37 shows a typical IV characteristic obtained after extensive baking. The discharge resistance is shown on Figure 38 from data obtained at a single temperature (1200°C) and pressure (135 torr). The lower and upper curves represent extremes obtained under different conditions of contamination and at different pressures. The upper curve corresponds to pressures above 140 torr and the lower to below 90 torr. At the lowest pressures and highest currents used (see Figure 37) the resistance fell to 250 Ω.

The temperature reached was almost independent of pressure and was controlled largely by the power deposited by the glow discharge. Figure 39 shows the temperature of copper beads within the discharge tube hot zone, as measured with an optical pyrometer, as a function of the input power.

Such a correlation of input power with temperature is consistent with a thermal conductivity of 50 10^{-4} W/cm °K for the insulation. Scaling of the thermal conductivity given by the manufacturer[19] to helium gives a similar mean value.* Clearly, the use of glow discharge heating can be treated analytically.

B. PULSED DISCHARGE

Pulsed discharges were applied to the 4" bore laser with the expected success. They were generally uniform and stable. Steady state conditions were reached very quickly, usually within three pulses, if the copper vapor density was high enough.

The importance of sufficient copper vapor density to high voltage discharge stability can be appreciated after a comparison of Figures 40 and 41.

Figure 40 shows the instability of the voltage across the pulsed discharge when the copper vapor density was relatively low (1.33 10^{14} cm^{-3}).

* Neon value is 20 x 10^{-4}.

FIGURE 37. CHARACTERISTIC OF GLOW DISCHARGE HEATER IN 4" BORE LASER PRESSURE WAS 40 TORR HELIUM

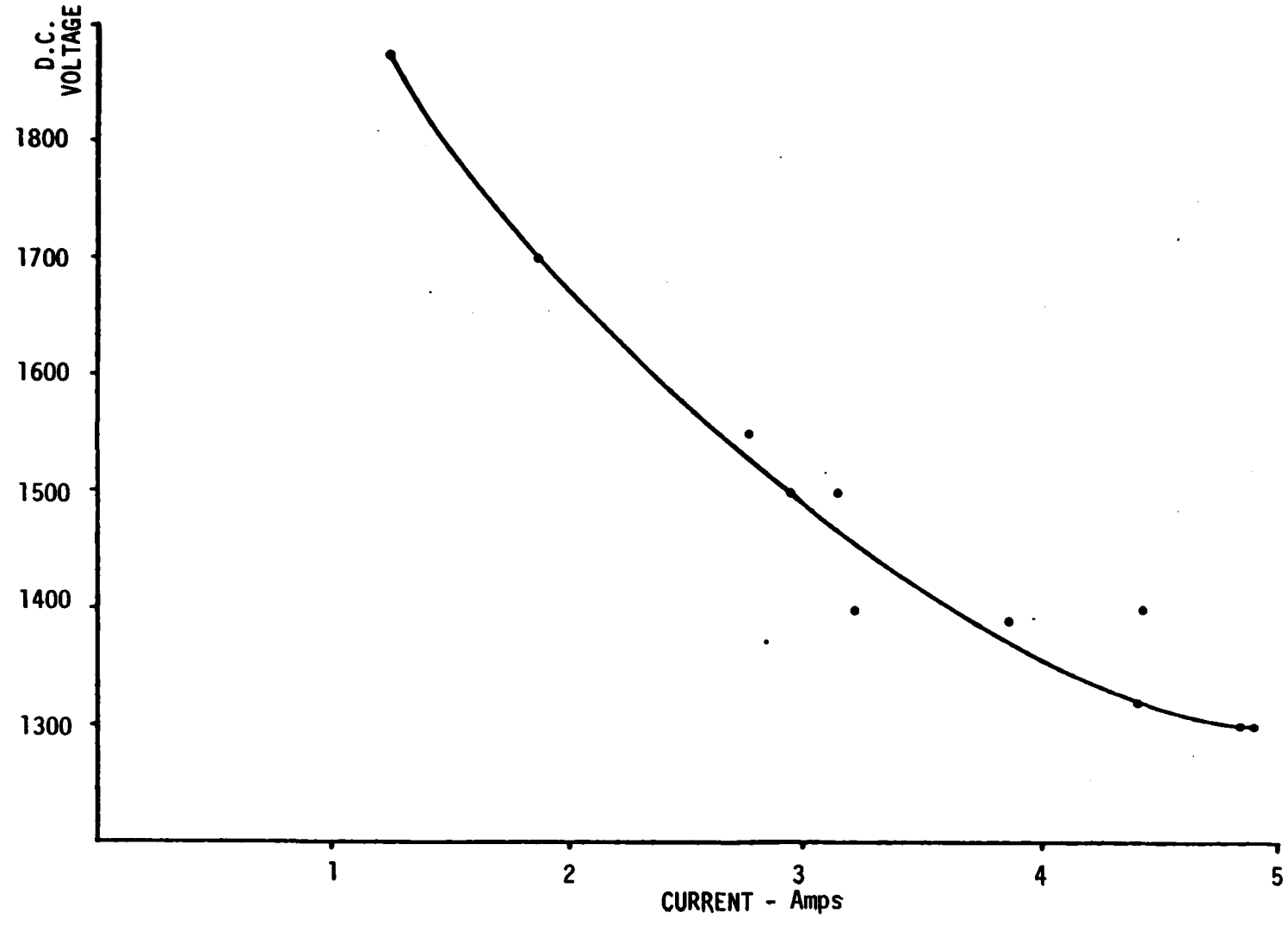

FIGURE 38. GLOW DISCHARGE RESISTENCE AS FUNCTION OF CURRENT

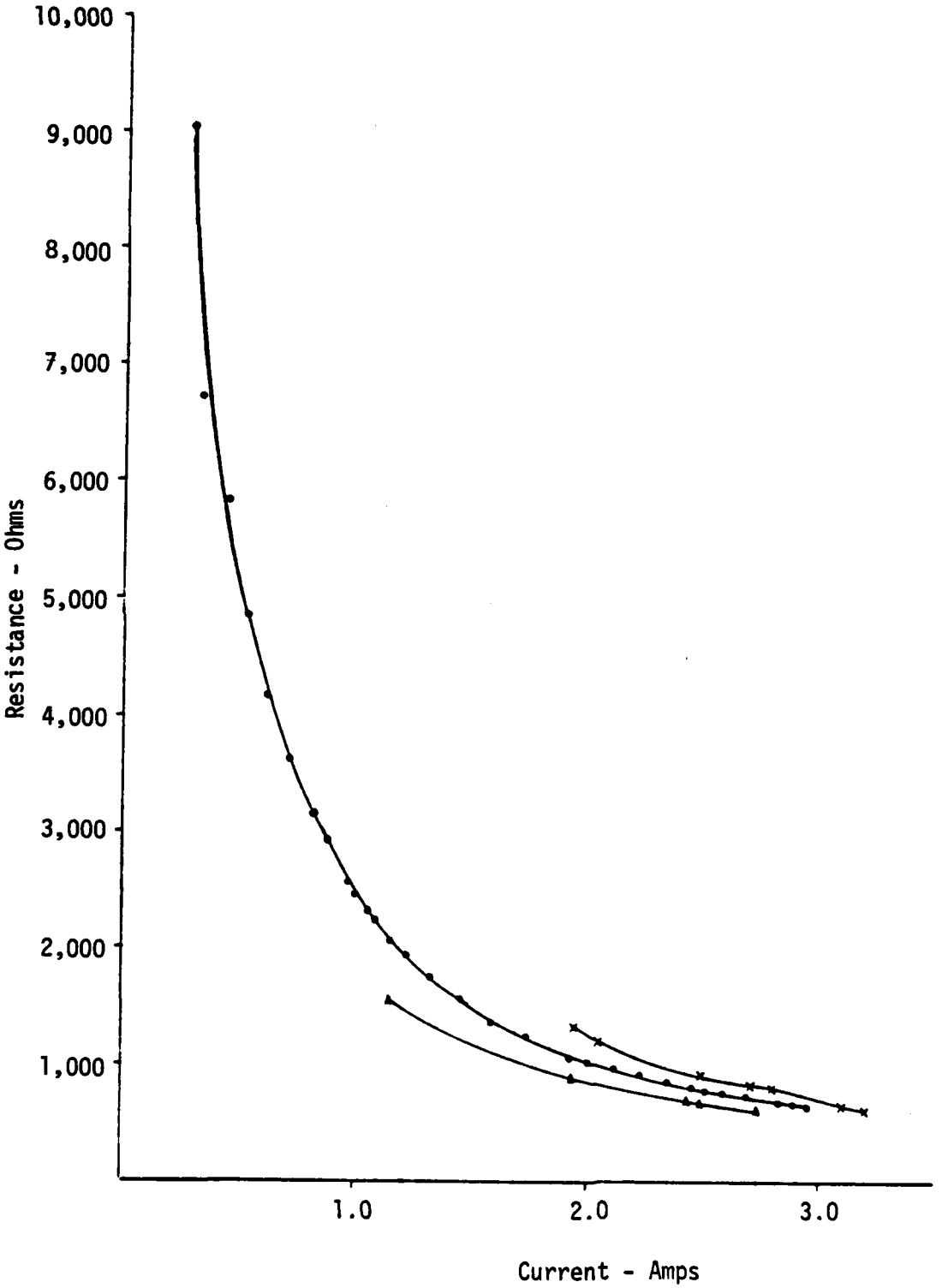

FIGURE 39. TEMPERATURE OF COPPER BEADS WITHIN 4" ID COPPER VAPOR LASER AS FUNCTION OF GLOW DISCHARGE INPUT POWER

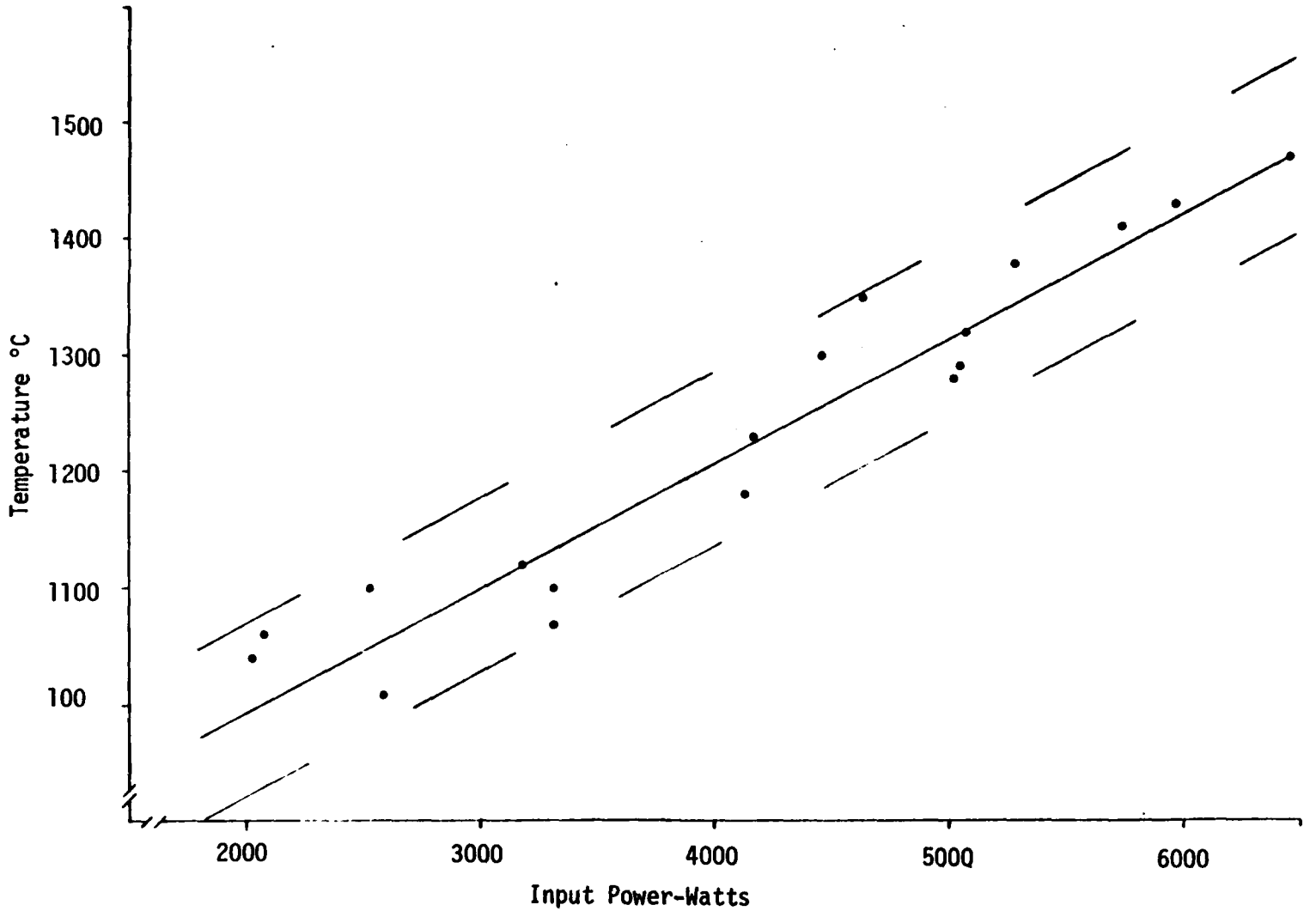

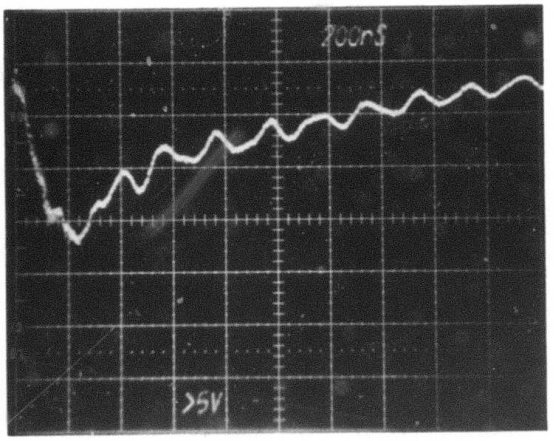

First Pulse
(a)

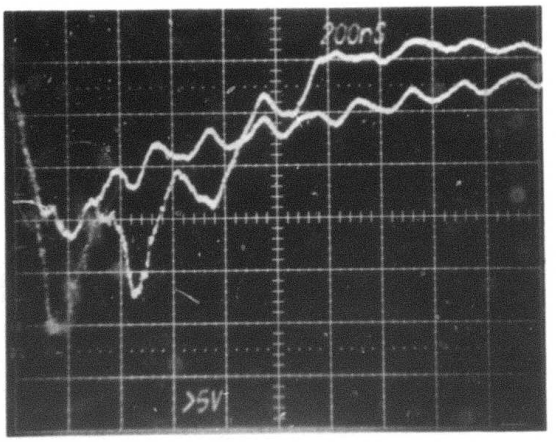

First Two Pulses
(b)

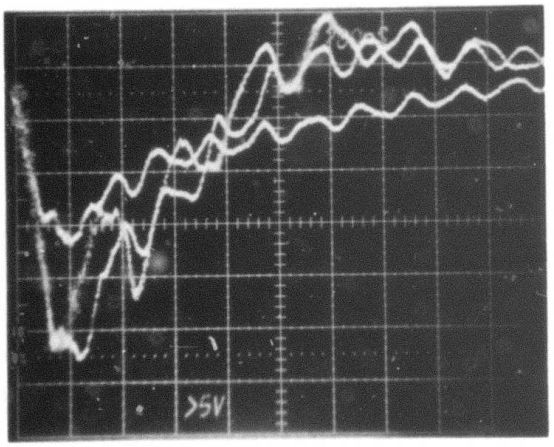

First Three Pulses
(c)

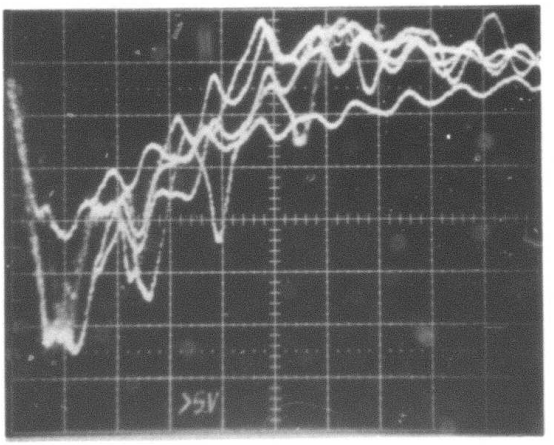

First Five Pulses
(d)

Amplitude: 5 kV/div

Sweep : 200 ns/div

FIGURE 40. TIME RESOLVED VOLTAGE DROP ACROSS 4" BORE LASER: 1310°C TUBE TEMPERATURE.

Power Supply Voltage	16.5 kV
Capacitor Peak Voltage	3.3 kV
Storage Capacitance	52.7 nf
Peaking Capacitance	23.8 nf
Specific Loading	3.65 mJ/cm^3
Repetition Rate	200 HZ

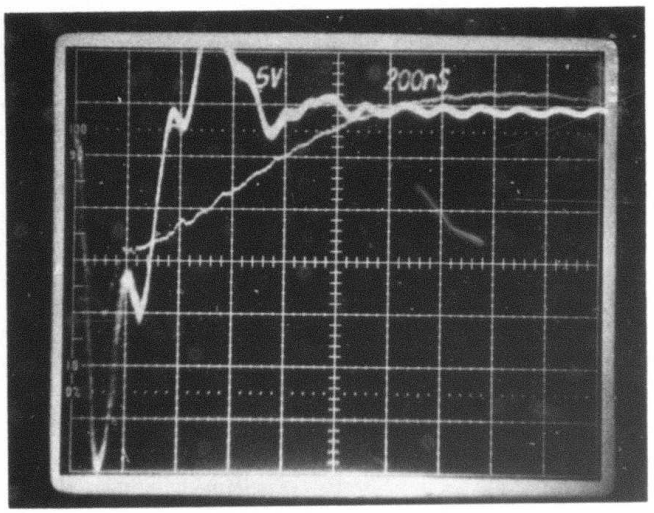

Amplitude: 5 kV/div
Sweep : 200 ns/div

First 14 Pulses

FIGURE 41. TIME RESOLVED VOLTAGE DROP ACROSS 4" BORE LASER: 1390°C TUBE TEMPERATURE

Power Supply Voltage	18 kV
Capacitor Peak Voltage	36 kV
Storage Capacitance	27.2 nf
Peaking	5.1 nf
Specific Loading	2.24 mJ/cm^3
Repetition Rate	200 HZ
Helium Pressure	38 torr

The first pulse was low, as expected, since doubling of the power supply voltage by the resonant charge circuit should only be seen on subsequent discharges. Furthermore, steady state ionization would not have yet built up. Near doubling of the power supply voltage was observed on the second pulse and there was a tendency for discharges after the third to be consistent during the first 300 ns of the discharge. However, thereafter the voltage changed a great deal from pulse to pulse. This in in strong contrast to observations with higher rate steady pulsed lasers where pulse to pulse reproducibility was high.

Increase of the copper vapor density to 3.6 10^{14} cm^{-3} stabilized the discharge considerably. As can be seen in Figure 41 and 42 (a), after the first pulse all subsequent pulses can be seen to overlay very nicely. Occasionally a change in discharge properties did occur later in a discharge pulse. Then, as can be seen on Figure 42 (b) one trace would exhibit reduced damping, due to reduced discharge resistance. The thyratron would then latch, as evidenced by a straight line on the oscilloscope trace.

It should be noted that the ringing period seen after the initial rise in Figures 41 and 42 is consistent with the capacitance, and a computed inductance (Figure 35) that assumes uniform current filling of the discharge tube. Any deviations from uniform filling of the discharge tube by the current would produce a change in the inductance and therefore this period would change. No such change in period can be seen in Figure 42 (b) and so the change in discharge properties is not one of significant constriction, in this case. Rather, it appears that during the first current reversal of one pulse the thyration did not shut off, leading to continued oscillation. The rapid decay of current during the first current reversal in the other pulses shows appropriate shut off. Evidently it is sometimes discharge properties within the thyration that cause the problem.

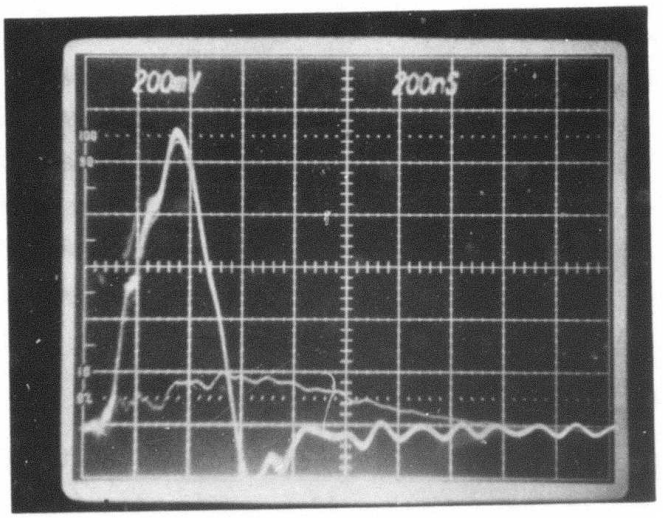

(a)

First 14 Pulses

Amplitude : 400 amps/div
Sweep : 200 ns/div

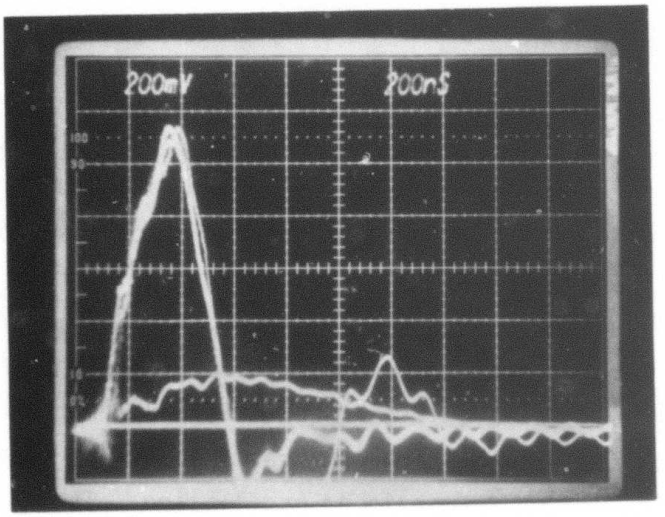

(b)

Thyratron Latching

FIGURE 42. TIME RESOLVED CURRENT THROUGH 4" BORE LASER : 1390°C TUBE TEMPERATURE.
SAME CONDITIONS AS FIGURE 41.

Discharge stability is, of course, dependent on some of the other discharge parameters. The stable discharge behavior shown on Figure 41 and 42 (a) was observed for both values of the storage capacitance used (27 and 51 nf) and so this is not a sensitive parameter. Reduction of the charging voltage to 20-25 kV caused instability of the discharge to return. Consequently, voltage is a sensitive parameter.

Thus, requirements for a stable discharge are consistent with requirements for high energy output as predicted by the computer simulation. Both a voltage of about 40 kV or greater and a copper vapor density of about 4 10^{14} cm^{-3} or greater are required. Large capacitance is not necessary and so its use may be wasteful.

C. LASING

Laser operation was obtained throughout the 4" laser bore as predicted. Of course, the size of the laser spot was a function of the copper vapor density and discharge voltage. Table 12 shows the dependence upon copper vapor density. As in smaller bore lasers, at low copper vapor densities the spot size was small and centered on the discharge tube axis. As the density was increased the spot grew to fill the tube. The largest spots appeared uniform in intensity when viewed through neutral density filters of different attentuation.

The most intense bursts were obtained with a 27 nf storage capacitor charged to 36 kV and discharged through a medium containing copper vapor density of 1.3 10^{15} cm^{-3} and helium buffer density of 20-40 torr. Each burst was composed of 13 pulses and produced a spot about 3 1/2" in diameter. One can estimate the pulse energy involved by noting that the spot was estimated by two experienced observers to have an intensity comparable to that of a 1-5 watt 1" diameter laser. Since the burst was .065 seconds long the eye should integrate properly and give this estimate some significance. Such laser intensity spread over a 3 1/2" circle would deposit 0.9-4J in .065 sec. Noting that only 12 of these thirteen pulses would contribute significantly to the output power one can estimate pulse energy of 166-331 mJ. This is consistent with the energy projected by the computer simulation model.

TABLE 12

DEPENDENCE OF LASER SPOT SIZE UPON COPPER VAPOR DENSITY

Copper Vapor Density	Laser Spot Diameter
$1.2\ 10^{14}\ cm^{-3}$	1"
$1.7\ 10^{14}$	2 1/2"
$5.9\ 10^{14}$	3 1/2"

The remaining time was not sufficient to make pulse energy measurements, operate in neon, or otherwise properly characterize the device.

D. COMPARISON WITH COMPUTER SIMULATION

A computer simulation with the CUHEI code was conducted for the experimental laser design (Table 10) operated with the parameters given on Figure 41. The simulated current and voltage drop are shown on Figure 43. Comparison with the experimental traces on Figures 41 and 42 shows excellent agreement. Note that the simulated voltage drop is actually across the peaking capacitor since that is actually where the measurement was made. The voltage drop across the discharge alone is experimentally inaccessible.

A CUHEI simulation was also conducted for the operating conditions that gave the best output the preceeding section (VI C). The total 51.05 nm and 578.2 nm pulse energy produced by the simulation was 74 mJ (53 mJ at 510.5 nm) and 21 mJ at 578.2 nm). This is consistent with the experimental estimates. It is significant to note that computer simulations with CUNEI using the same input parameters, except a neon buffer gas, yielded an output of almost .25 joules (32 $\mu J/cm^{-3}$).

As pointed out earlier, electron density decays substantially during the long interpulse period. This can be seen on Figure 44, to produce a minimum of 1.7×10^{12} cm^{-3}. It should be compared to our results on Figure 13 and the results of Kushner and Warner where at 5 KHZ rates there is comparative little decay. The minimum there is about 2×10^{14} cm^{-3}. This later minimum is above even the maximum obtained at low repetition rates (Figure 44).

Consequently, at low repetition rates the electron density must rise dramatically during discnarge build up (Figure 45). That takes place in such a way that during the time of maximum power deposition and lasing the density is only about 3-4 10^{13}. This is about an order of magnitude below that of high repetition rate operation and so leads to three times larger skin depth.

Thus, the discharge at low rates represents more of a repetitive breakdown than at high rates where it can be looked upon as repetitive heating of a steady state plasma. Higher voltages are, of course, necessary to produce a reliable breakdown and higher copper vapor densitites will reduce the required breakdown voltage, as was observed.

FIGURE 43. SIMULATED CURRENT AND VOLTAGE DROP FOR 4" BORE LASER. SAME CONDITIONS AS FIGURE 41.

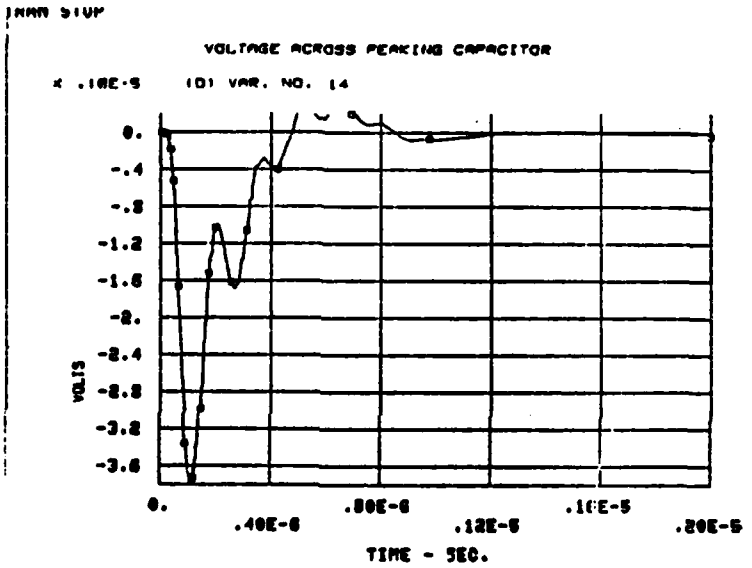

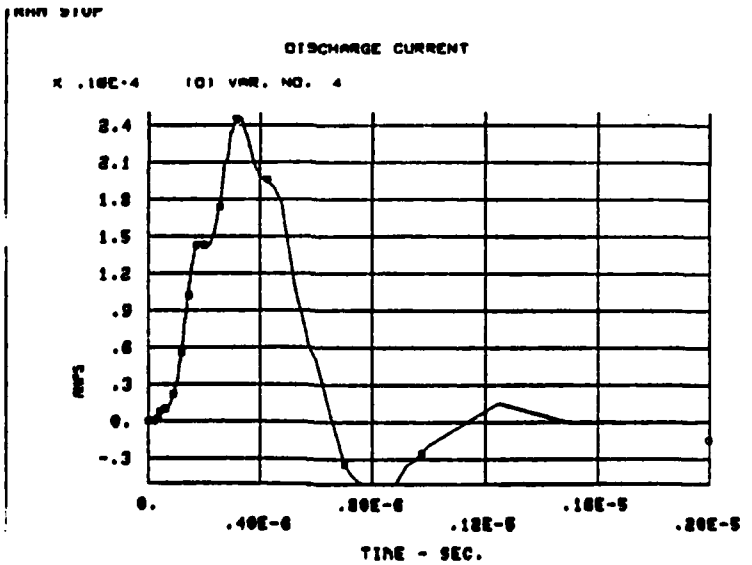

Figure 44. Decay of Electron Density During Interpulse Period of 200 HZ Operation. Conditions are the same as on Figure 41.

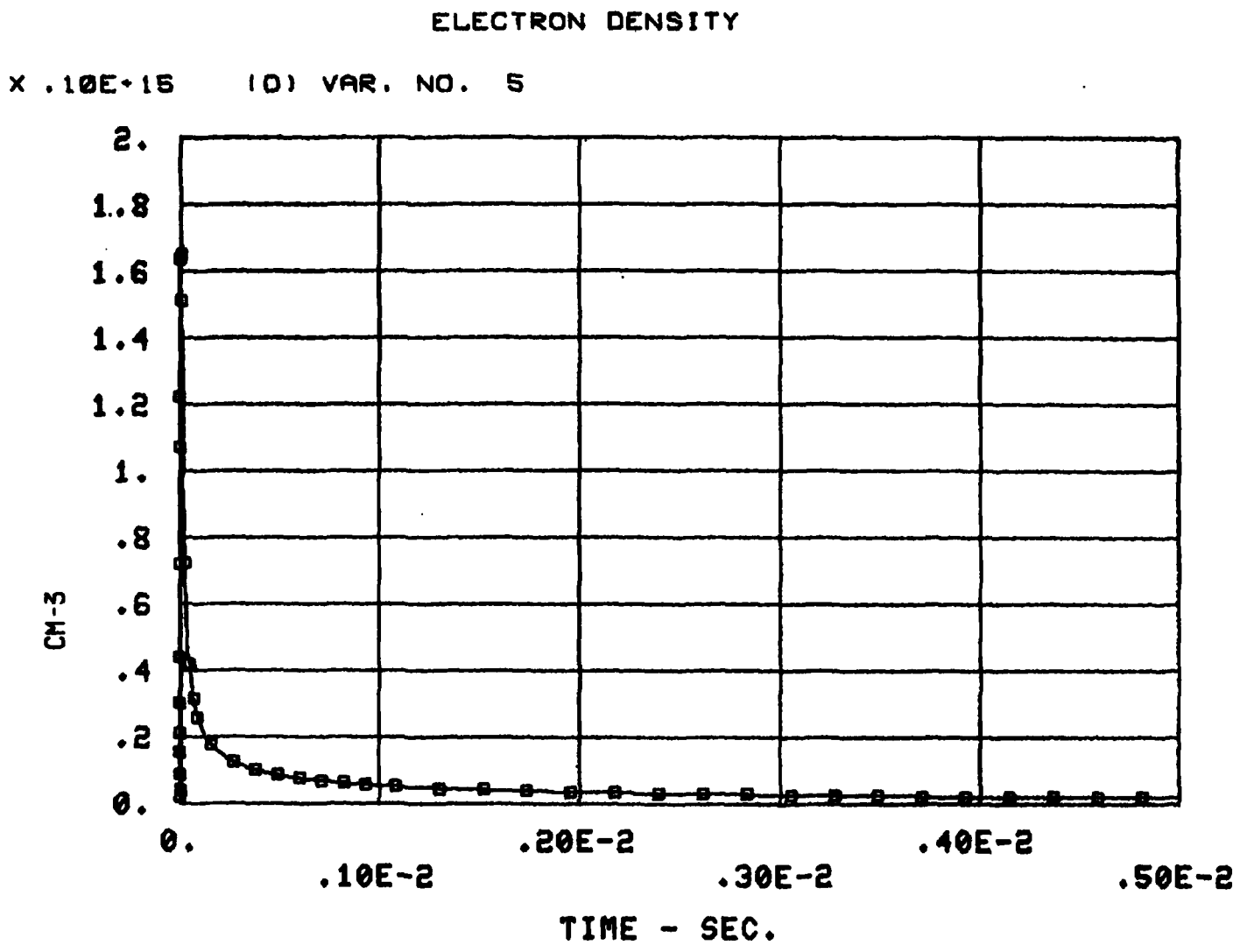

Figure 45. Build up of Electron Density as Discharge Develops. Conditions are the same as Figure 41 and 44.

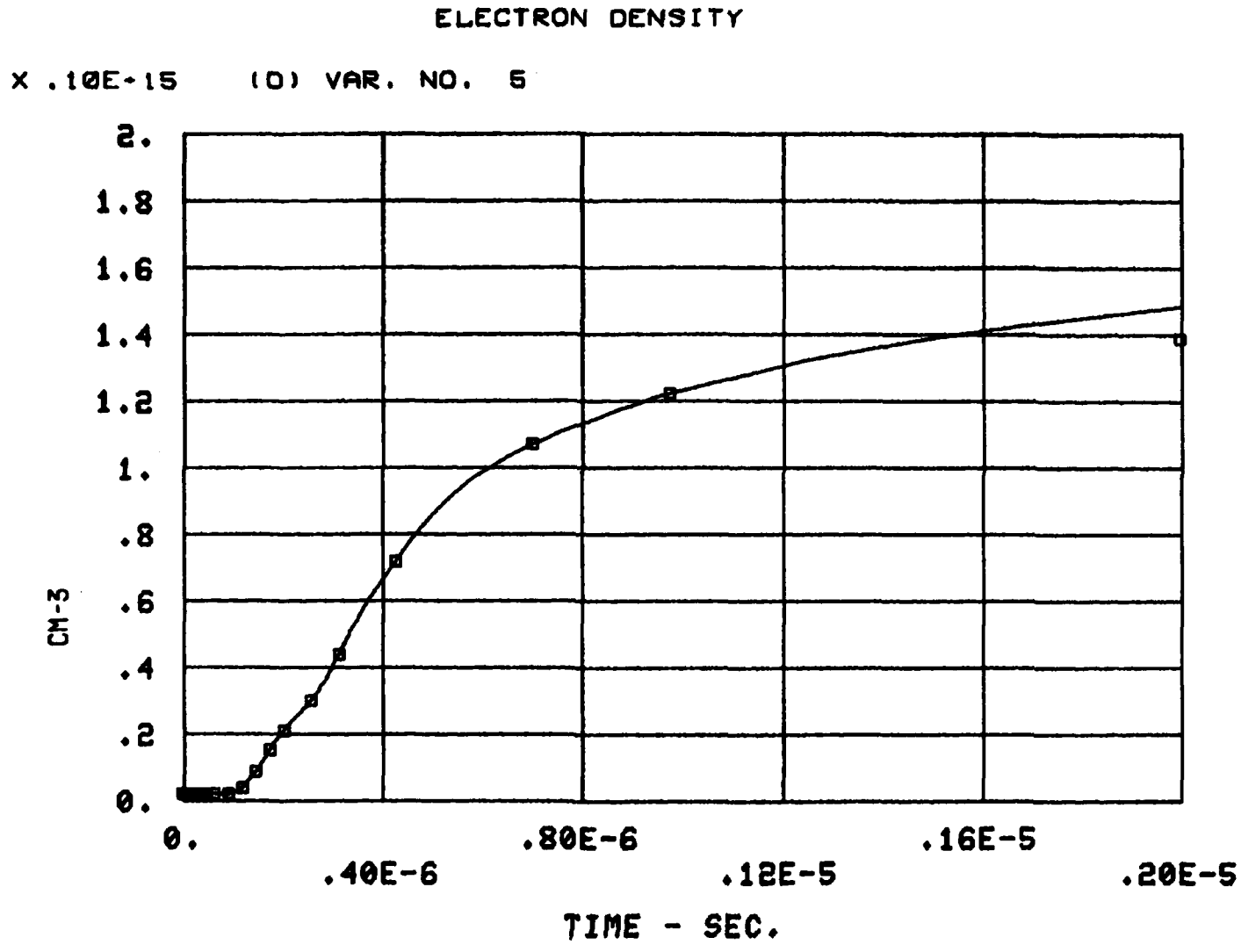

VII. SUMMARY AND CONCLUSIONS

The CUHEI and CUNEI computer models were developed for simulation of copper vapor lasers operating in helium and neon buffer gases. They were both validated with data from high repetition rate experiments.

The CUNEI model was then used to determine the dependence of output upon various parameters in a neon buffered, 10 cm bore, low repetition rate device. Optimum output was obtained at lower repetition rates when higher voltages were used. At a given rate output increased most strongly with increased voltage. Optimum values were found for other parameters. Some of the best results corresponded closely to early empirical projections.

An optimized output of up to .33J was simulated with 1.8% efficiency at 200 HZ rate. With other parameters 2.5% efficiency was simulated.

The key to this mode of operation is the decay of electron density that takes place during long interpulse periods. At high repetition rates very little decay takes place and plasma shielding effects can be observed.[9] At low rates electron densities are lower, higher voltages must be used, and plasma shielding effects are minimized. The contrast may be viewed as between pulsed heating of a steady state plasma and repetitive breakdown of a well preionized medium. The extreme of operation with inadequate preionization must, of course, be avoided but with the voltages of interest here rates as low as 10-20 HZ should be permissible.

A flexible test facility was built based upon these computer predictions. The design used a D.C. glow discharge to heat a 4 1/8" ID laser tube and bursts of high voltage discharge pulses to excite the laser transition. This allowed the laser to be heated to 1500°C and discharge voltages of up to 50 KV to be tested. The technology developed here was quite successful and should be of use in heating and testing a large variety of metal vapor lasers.

Reliable discharges and lasing were obtained at 200 HZ in helium throughout the full bore of the laser. Resulting current and voltage waveforms agreed closely with CUHEI computer simulations.

In addition, estimates of the best pulse energy obtained, were in the range of > 70 millijoules and are consistent with computer model simulations of 74 mJ. Though unoptimized this is well above the highest pulse energy previously reported. Specific output is about 10 $\mu J/cm^{-3}$ similar to that commonly obtained from small helim buffered lasers. Clearly volume sealing was successful.

Time was not sufficient to conduct optimization or measurements of the helium buffered device. Even preliminary lasing was not attempted in a neon buffer.

Nonetheless, the agreement already obtained with the computer simulations of this large bore device leads us to expect that the optimized simulations of over .25 Joules are realizable experimentally. All that is necessary is operation of the present device in neon with parameters identical to those already used.

Finally, the model of operation at low repetition rates was also supported by several other observations, notably the dependence of discharge reliability on voltage and copper vapor density and the uniformity of the laser spot indicating absence of skin depth effects. Thus, this mode of operation should be effective in discharge tubes of considerably larger diameter. Pulse energies have been simulated of about a joule from a single 6" bore oscillator.[15]

Scaling of copper vapor laser operation has thus been supported to the 100 mJ level with strong indications of at least an order of magnitude further improvement being possible.

REFERENCES

1. T. W. Karras, et al, "Advanced Pulsed Metal Vapor Laser Designs", General Electric Co., TIS-80SDS031, December 1980.

2. W. T. Walter, N. Solimene, M. Piltch and G. Gould, "Efficient Pulsed Gas Discharge Lasers", IEEE J. Quart. Elect. QE-2 474 (1966).

3. J. L. Miller and T. Kan, "Metastable Decay Rates in a Cu-Metal-Vapor Laser", J. Appl. Phys. 50 3849 (1979).

4. B. G. Bricks, T. W. Karras, T. E. Buczacki, L. S. Springer and R. S. Anderson, "High Repetition Rate Flowing Copper Vapor Laser", IEEE J. Quart. Elect. QE-11 57 (1975).

5. P. A. Bokhan, V. A. Gerasimov, V. I. Solomonov and B. V. Schleglov, "Stimulated Emission Mechanism of a Copper Vapor Laser", Sov. J. Quart. Elect. 8 1220 (1978).

6. R. S. Anderson, B. E. Warner, C. Larson, and R. E. Grove, CLEO-81, Digest of Technical Papers, 10-12 June 1981 (IEEE/OSA), p. 50.

7. C. S. Liu, D. W. Feldman, John L. Pack and L. A. Weaver, "Kinetic Processes in Continuously Pulsed Copper Halide Lasers", IEEE j. Quant. Electron QE-13, 744 (1977).

8. P. A. Bokhan, V. I. Silant'ev and V. I. Solomonov, "Mechanism for Limiting the Repetition Frequency of Pulses from a Copper Vapor Laser:, Sov. J. Quant. Electron 10 724 (1980).

9. M. J. Kushner and B. E. Warner, "Large-Bore Copper-Vapor Lasers: Kinetics and Scaling Issues". UCRL 88517 Preprint December 1982.

10. M. J. Kushner, "A Self Consistent Model for High Repetition Rate Copper Vapor Lasers", IEEE J. Quart. Electron QE-17, 1555 (1981).

11. General Electric Model 6-15 Copper Vapor Laser Instruction Manual (1980).

12. T. W. Karras, "Copper Vapor Lasers: A Review", AGARD 29th Symposium Conference, Proceedings (No. 300), Special Topics in Optical Propagation, Monterey, CA (1981).

13. B. E. Warner and M. J. Kushner, "Controlling Kinetic Parameters of 100 Watt Large Bore Copper Vapor Lasers," Proceedings of the International Conference on Lasers '81, Ed. by C. Collins STS Press 1982.

14. C. E. Anderson et al, "High Power Copper Vapor Laser Development," Final Report to LLNL Contract P. O. 4946809 (1981).

15. T. W. Karras, et al, "Copper Vapor Laser Amplifier Study," GE TIS No. 82SDS019, September 1982.

16. S. Gabay, I. Smilanski, and Z. Karny, "Externally Heated Copper Vapor Laser for Parametric Studies," IEEE J. Of Quant. Electron QE 18, 996 (1982).

17. J. J. Kim and J. Covey, "High Temperature Insulation for the Copper Vapor Laser" Rev. Sci. Inst. 53, 1623(1982).

18. T. W. Karras, "Contaminants in Metal Vapor Lasers" in Proceeding of the International Conference on Lasers '80, Ed. by C. Collins, STS Press (1981).

19. Zircar Corp. Florida, N.Y.

20. Observations of Zirconia Alumina Reactions at 1400°C-1450°C were also observed by T. Alger at Lawrence Livermore National Laboratory.

21. S. V. Panshkin "Contraction of Current Carrying Plasma" High Temp. 10 1058 (1972).

22. R. Turner "The Glow to Arc Transition in a Pulsed High-Pressure Gas Discharge" J. Appl. Phys. 52 681 (1981).

23. G. N. Gerasimov, "Contraction of an Electric Discharge in Inert Gases at Medium Pressures" Optics and Spect. 43 209 (1977).

24. T. W. Karras, "Glow Discharge Heating", GE PIR 1250-PFI-E7-300, October 1981.

25. L. W. Springer, T. W. Karras, R. S. Anderson and B. G. Bricks. "Discharge Circuitry for High Repetition Rate Metal Vapor Lasers", Proceedings IEEE International Pulsed Power Conference, Lubbock, Texas 1976 (76-CH1147-8).

26. Private communication R. F. Caristi, EG&G.